2

NAVAL POSTGRADUATE SCHOOL

Monterey, California

THESIS

EVALUATION OF THE COMPUTATIONAL VALIDITY OF THE IMAGE MODEL IN PREDICTING THE SOUND FIELD IN A WEDGE-SHAPED LAYER USING ACOUSTICAL RECIPROCITY

by
Lee, Kyung Taek
December 1991

Co-Advisor: Alan B. Coppens
Co-Advisor: James V. Sanders

Approved for public release; distribution is unlimited

Unclassified
SECURITY CLASSIFICATION OF THIS PAGE

REPORT DOCUMENTATION PAGE

1a. REPORT SECURITY CLASSIFICATION UNCLASSIFIED	1b. RESTRICTIVE MARKINGS
2a. SECURITY CLASSIFICATION AUTHORITY	3. DISTRIBUTION/AVAILABILITY OF REPORT Approved for public release; distribution is unlimited.
2b. DECLASSIFICATION/DOWNGRADING SCHEDULE	
4. PERFORMING ORGANIZATION REPORT NUMBER(S)	5. MONITORING ORGANIZATION REPORT NUMBER(S)
6a. NAME OF PERFORMING ORGANIZATION Naval Postgraduate School 6b. OFFICE SYMBOL *(If applicable)* DH	7a. NAME OF MONITORING ORGANIZATION Naval Postgraduate School
6c. ADDRESS *(City, State, and ZIP Code)* Monterey, CA 93943-5000	7b. ADDRESS *(City, State, and ZIP Code)* Monterey, CA 93943-5000
8a. NAME OF FUNDING/SPONSORING ORGANIZATION 8b. OFFICE SYMBOL *(If applicable)*	9. PROCUREMENT INSTRUMENT IDENTIFICATION NUMBER
8c. ADDRESS *(City, State, and ZIP Code)*	10. SOURCE OF FUNDING NUMBERS Program Element No. / Project No / Task No / Work Unit Accession Number

11. TITLE *(Include Security Classification)*
EVALUATION OF THE COMPUTATIONAL VALIDITY OF THE IMAGE MODEL IN PREDICTING THE SOUND FIELD IN A WEDGE-SHAPED LAYER USING ACOUSTICAL RECIPROCITY.

12. PERSONAL AUTHOR(S) Lee, Kyung Taek (ROK Navy)

13a. TYPE OF REPORT	13b. TIME COVERED	14. DATE OF REPORT *(year, month, day)*	15. PAGE COUNT
Master's Thesis	From To	December 1991	56

16. SUPPLEMENTARY NOTATION
The views expressed in this thesis are those of the author and do not reflect the official policy or position of the Department of Defense or the U.S. Government.

17. COSATI CODES			18. SUBJECT TERMS *(continue on reverse if necessary and identify by block number)*
FIELD	GROUP	SUBGROUP	Image Method, Wedge-Shaped layer, reciprocal Position

19. ABSTRACT *(continue on reverse if necessary and identify by block number)*

Computer models based on the method of image were used to investigate and calculate the pressure amplitude distribution in wedge-shaped (tapered) water layer overlying a fast, absorbing bottom. The pressure amplitude of the field was generated and compared at reciprocal positions of source and receiver. The results showed that the ratio of pressure difference to the pressure was larger when the position of source or receiver was closer to the bottom and nearer the apex.

20. DISTRIBUTION/AVAILABILITY OF ABSTRACT ☒ UNCLASSIFIED/UNLIMITED ☐ SAME AS REPORT ☐ DTIC USERS	21. ABSTRACT SECURITY CLASSIFICATION Unclassified
22a. NAME OF RESPONSIBLE INDIVIDUAL Prof. Alan B. Coppens	22b. TELEPHONE *(Include Area code)* (408) 646-2116 22c. OFFICE SYMBOL PH/SD

DD FORM 1473, 84 MAR — 83 APR edition may be used until exhausted. All other editions are obsolete

SECURITY CLASSIFICATION OF THIS PAGE
Unclassified

Approved for public release; distribution is unlimited.

Evaluation of the computational validity of the image model in predicting the sound field in a wedge-shaped layer using acoustical reciprocity

by

Lee, Kyung Taek
LT, ROK Navy

B.S., Naval Academy 1986

Submitted in partial fulfillment
of the requirements for the degree of

MASTER OF SCIENCE IN ENGINEERING ACOUSTICS

from the

NAVAL POSTGRADUATE SCHOOL
December 1991

Author: ______________________
Lee, Kyung Teak

Approved by: ______________________
Alan B. Coppens, Co-Advisor

____
James V. Sanders, Co-Advisor

____
Anthony A. Atchley, Chairman
Engineering Acoustics Academic Committee

ABSTRACT

A computer model based on the method of images was used to investigate and calculate the pressure amplitude distribution in a wedge-shaped (tapered) water layer overlying a fast, absorbing bottom. The pressure amplitude of the field was generated and compared at reciprocal positions of source and receiver. The results showed that the ratio of pressure-difference to the pressure when the position of source or receiver was more near the bottom, that is, deeper and more near the apex.

TABLE OF CONTENTS

LIST OF TABLES

LIST OF FIGURES

ACKNOWLEDGMENT

First of all, I want to express my sincere appreciation to God and give Him all the glory as He has taken care of me and kept me in right direction since my arrival.

I wish to thank my thesis advisors, Alan B. Coppens and James V. Sanders for their helping and understanding me to complete my thesis. I would also like to thank the professors in Acoustics for teaching and giving scholarly advise and Korean professors who are teaching here for helping and supporting my academic life.

I wish to thank fellow Korean students and their family and wonderful friends in Young Nak church for supporting and encouraging my personal life.

Finally, I would like to express my deepest thanks to my parents, Lee Yeong Uk and Park Boung Ok, and my family of brother, my sister and my future wife for their everlasting support, praying and encouraging for successful study.

I. INTRODUCTION

Propagation of sound radiated from a source in an ocean with a sloping bottom has received considerable attention during recent years for both theoretical reasons and applications to underwater sound. Many scientists [Ref.1-11] have researched this subject and created a number of acoustic models to predict the sound field within a wedge-shaped fluid overlying a penetrable or a rigid fluid bottom.

Considering practical interest for underwater acoustics, a limitation of the ideal wedge model of the ocean lies in the boundary conditions: The top boundary may be approximated as an impenetrable, pressure-release surface, but the bottom of a real ocean wedge is not usually a perfect reflector. It can be considered as a fast bottom, that is, a water fluid sediment interface that shows a critical grazing angle.

The acoustic field in a wedge shaped shallow water duct with ideal boundary conditions has been studied by Bradley and Hudimac [Ref. 1]. They have analyzed the case of an isospeed duct with one pressure release and one rigid surface. The theoretical analysis has been carried out in both image theory and normal mode theory.

pressure amplitude and phase in the upslope direction along the bottom of wedge-shaped fluid layer overlying a fast fluid bottom.

Jensen and Kuperman [Ref. 4] used the parabolic equation model to study the model cut off during upslope propagation in a wedge-shaped ocean and made comparison between experiment and theory in 1980.

In 1982, Lee and Botseas [Ref. 5] used an Implicit Finite-Difference (IFD) computer model, that is problems arise when the fourier transform encounters an interface between two medium having different sound speed and densities, to solve the parabolic equation.

In 1983, Jager [Ref. 6] developed IFD program that incorporates exact interface conditions which are preserved for horizontal and sloping interfaces along a user-specified bottom profile for solving the parabolic equation.

The sound field in an absorbing fluid substrate underlying a wedge-shaped fluid with high sound speed has been studied by Coppens, Sanders, and Humphries in 1984. [Ref. 7]

In the same year, Baek [Ref. 8] used the computer model based on the method of image to predict pressure amplitude and phase distribution in a wedge-shaped medium overlying a fast absorbing bottom.

Lesesne [Ref. 9] also studied and compared two computer models developed by Coppens and Sanders which is not limited to up or downslope direction.

In this research, I will use computer model for image method that was programmed in Fortran for use on the NPS IBM 3033 computer main frame to calculate the pressure field in a wedge-shaped ocean with a pressure release surface and an acoustically fast bottom.

This computer program was developed by LTJG George Nassopoulos(Greece Navy). The outputs will be compared at reciprocal positions of source and receiver and be analyzed for the evaluation of the validity of the image model in above conditions.

II. THEORY

The following development is a summary of previous research of J.V.Sanders, A.B.Coppens and their students at the Naval Postgraduate School.

The complex acoustic pressure in the wedge from the point source can be determined by using the method of images. The assumption of constant sound speed in each of the two different mediums makes the method of images an appropriate approach for predicting the sound field.

In the method of images, the reflections of sound from boundaries are replaced by images of the source that reproduce the effects of the interactions with the boundaries. For the wedge-shaped layer, images lie on a circle whose center is the apex of the wedge. The source and each of image radiates a spherical wave of the appropriate phase. The total pressure and phase at any field point within the wedge is found by the phase-coherent summation of these waves. Higher images correspond to more reflections from the bottom so the pressure distribution of these higher images decrease progressively.

A typical three-dimension geometry for wedge is shown in Figure 1. The following definition and symbols for source and receiver parameters apply and will be used throughout.

β	=	wedge angle
R_1	=	normalized distance from apex to source
R_2	=	normalized distance from apex to receiver
Y_o	=	normalized distance along the shore between receiver and source
γ	=	source angle measured upward from the interface
δ	=	receiver angle measured upward from the interface
D1	=	the ratio of medium density to bottom density (ρ_1/ρ_2)
CC	=	the ratio of the speed of sound in the medium to the speed of sound in the bottom (C_1/C_2)
θ_c	=	critical angle for the bottom
X	=	normalizing distance
α/K_2	=	wave number in the bottom divided into the absorption in the bottom (loss term)

For the fast bottom, all distances are normalized to the dump distance x measured from the apex along the wedge interface at which the lowest mode attains cut off. The following formula is applied,

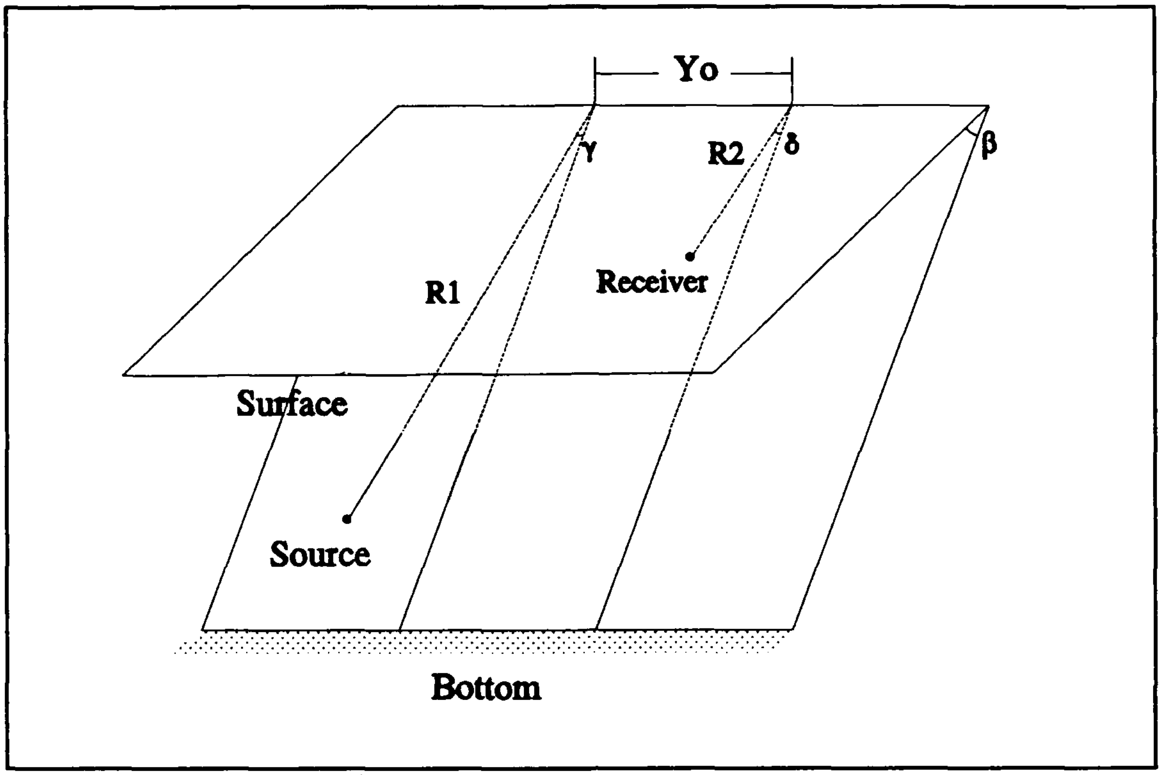

Figure 1. Three-Dimensional Wedge Geometry

$$K_1X=\frac{\pi}{2\sin\theta_c\tan\beta}$$

The normalized range is used in the image method program. For this model, we use wedge angles of the from π/N where N is an integer and consequently no apex term exists. [Ref. 2]

Then, the number of images in upper or lower half-space is

$$N=[\frac{180}{\beta}]$$

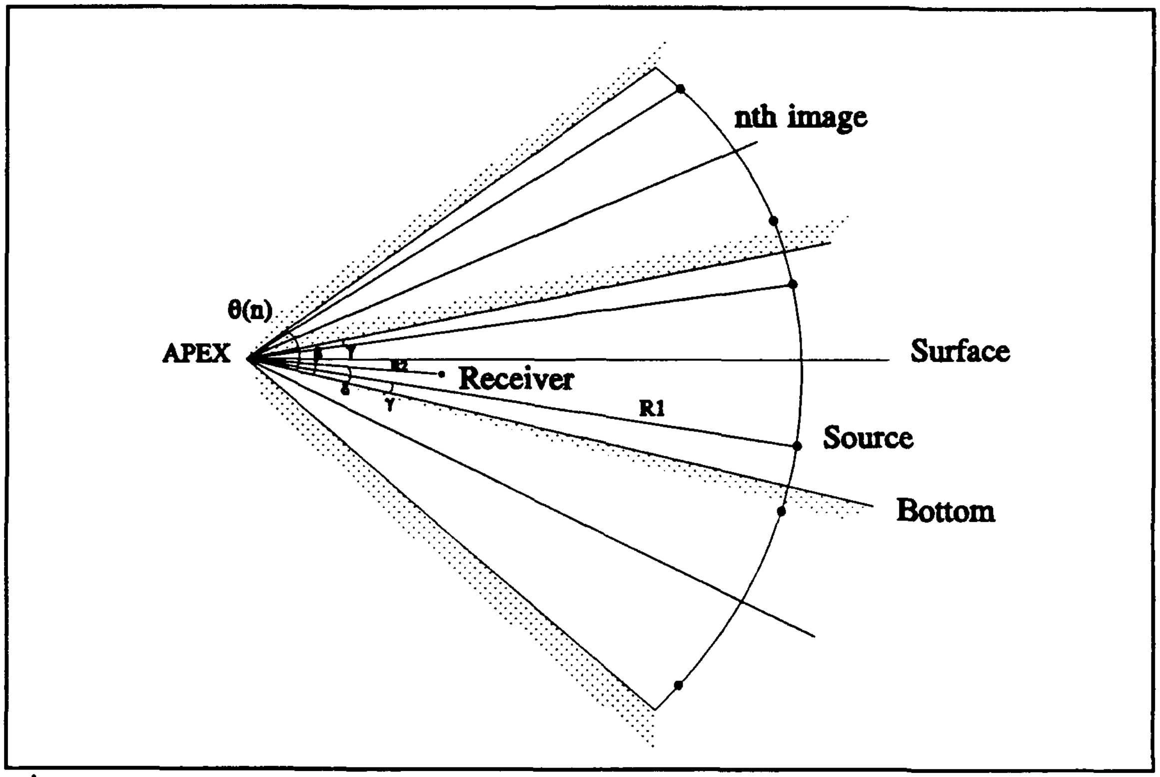

Figure 2. Image Structure for a Wedge-Shaped Layer

In Figure 2, the relationship between the receiver and the n^{th} source is represented and the angle θ_n of the n^{th} image, measured from the bottom, is given by:

$$\theta_n = \beta(n-1)+\gamma \quad , \quad \text{for n odd}$$

$$\theta_n = \beta_n - \gamma \quad , \quad \text{for n even}$$

Figure 3 shows the distance between the receiver and the n^{th} image;

$$(R')^2 = R_1^2 + R_2^2 - 2R_1R_2\cos(\theta_n - \delta)$$

$$R(n) = \sqrt{(R')^2 + Y_0^2} = \sqrt{R_1^2 + R_2^2 - 2R_1R_2\cos(\theta_n - \delta) + Y_0^2}$$

for the upper group of images, and

$$(R')^2 = R_1^2 + R_2^2 - 2R_1R_2\cos(\theta_n + \delta)$$

$$R'(n) = \sqrt{R_1^2 + R_2^2 - 2R_1R_2\cos(\theta_n + \delta) + Y_0^2}$$

for the lower group of images.

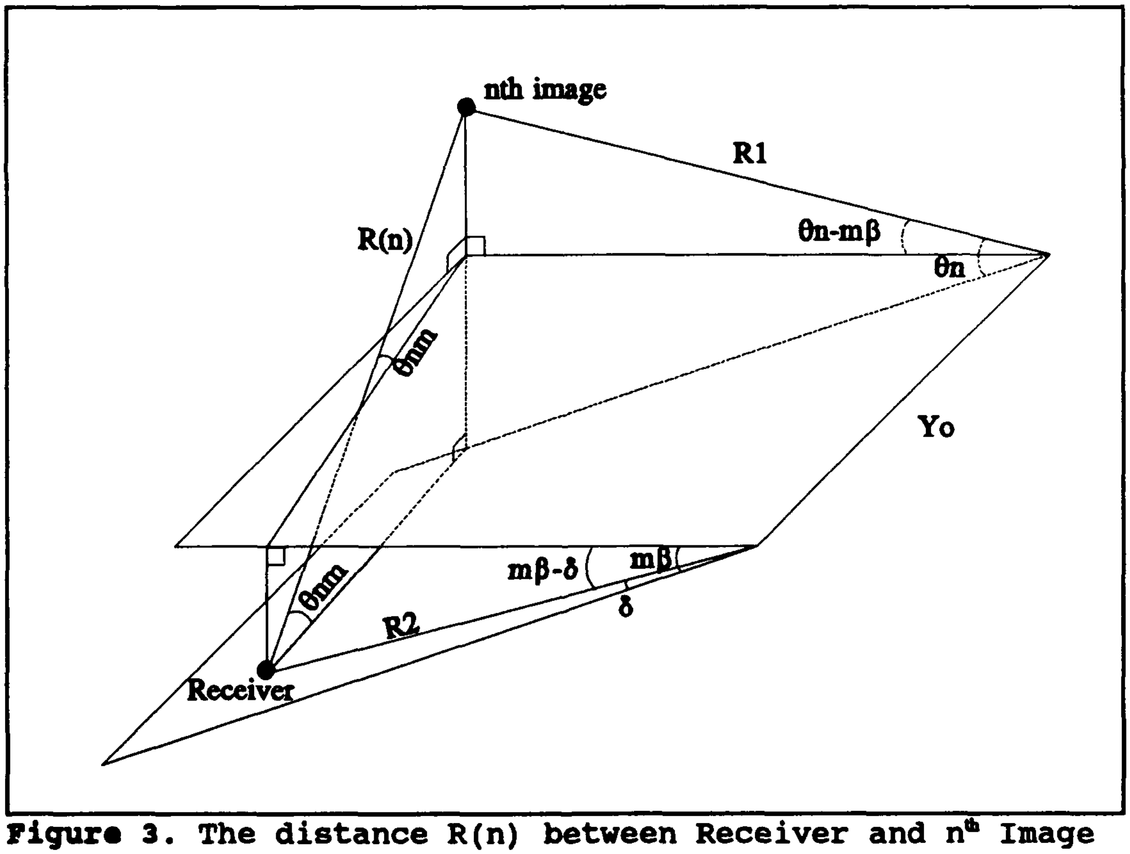

Figure 3. The distance R(n) between Receiver and n[th] Image

The number of times of the relevant reflection along the path from image to receiver is equal to the number of times the path interacts the bottom and its images. The total reflection coefficient is the product of all reflection coefficients along the path from the specific image to the receiver.

The reflection coefficient for the n_{th} image at the m_{th} bounce can be approximated by the plane wave reflection coefficient, if the distance from the source to the point on the bottom at which the initial bounce takes place is large compared to wave length in the wedge.

The reflection coefficient is;

$$R_{nm}=\frac{\frac{\rho_2 c_2}{\rho_1 c_1}-\psi_{nm}}{\frac{\rho_2 c_2}{\rho_1 c_1}+\psi_{nm}}$$

where

$$\psi_{nm}=\frac{\sqrt{1-(\frac{c_2}{c_1})^2\cos^2\theta_{nm}}}{\sin\theta_{nm}} \quad , \qquad \theta_{nm}\geq\theta_c=\cos^{-1}(\frac{c_1}{c_2})$$

With a lossy bottom, the above can be generalized with the help of

$$\frac{c_1}{\tilde{c}_2}=\frac{c_1}{c_2(1-j\frac{\alpha}{k_2})}\approx\frac{c_1}{c_2}(1+j\frac{\alpha}{k_2})$$

and

$$(\frac{c_1}{\tilde{c}_2})^2\approx(\frac{c_1}{c_2})^2+2j(\frac{c_1}{c_2})^2\frac{\alpha}{k_2}$$

The result[Ref. 15] is

$$R_{nm}=\frac{\frac{\rho_2}{\rho_1}\sin\theta_{nm}-\sqrt{(\frac{c_1}{\tilde{c}_2})^2-\cos^2\theta_{nm}}}{\frac{\rho_2}{\rho_1}\sin\theta_{nm}+\sqrt{(\frac{c_1}{\tilde{c}_2})^2-\cos^2\theta_{nm}}}$$

$$=\frac{\frac{\rho_2}{\rho_1}\sin\theta_{nm}-\frac{1}{\sqrt{2}}\sqrt{\sqrt{b^2+a^2}+a}+j\frac{1}{\sqrt{2}}\sqrt{\sqrt{b^2+a^2}-a}}{\frac{\rho_2}{\rho_1}\sin\theta nm+\frac{1}{\sqrt{2}}\sqrt{\sqrt{b^2+a^2}+a}-j\frac{1}{\sqrt{2}}\sqrt{\sqrt{b^2+a^2}-a}}$$

where

$$a=(\frac{c_1}{c_2})^2-\cos^2\theta_{nm},\ b=2(\frac{c_1}{c_2})^2\frac{\alpha}{k_2}$$

So, the angle of incidence must be determined to find a reflection coefficient.

The angle of incidence θ_{nm} of the upper n^{th} image on the m^{th} plane is shown in Figure. 4:

$$Sin(\theta_{nm}) = \frac{R_1 \sin(\theta_n - 2m\beta) + R_2 \sin(2m\beta - \delta)}{R(n)}, \quad m=1,\ 2,\ 3,...M$$

for the upper image,

$$Sin(\theta'_{nm}) = \frac{R_1 \sin(\theta'_n - 2m\beta) + R_2 \sin(2m\beta + \delta)}{R'(n)}, \quad m=0,\ 1,\ 2,\ ...M$$

for the lower image.

In these expressions the index m indicates each bottom plane and the number M is the total number of bottom the sound interact with along path from source to receiver;

$$M = INT\ [\frac{\theta_n}{\beta}] = INT\ [\frac{n-1}{2}]$$

The complex acoustic pressure at the arbitrary position is the summation of the complex pressure from every image which consist of the contribution from the direct path, the images above the wedge and the image below the wedge. In this program, upper family of images include the direct path. So, we don't need to calculate the reflection coefficients for the first and second images among upper images because these don't interact with any bottom.

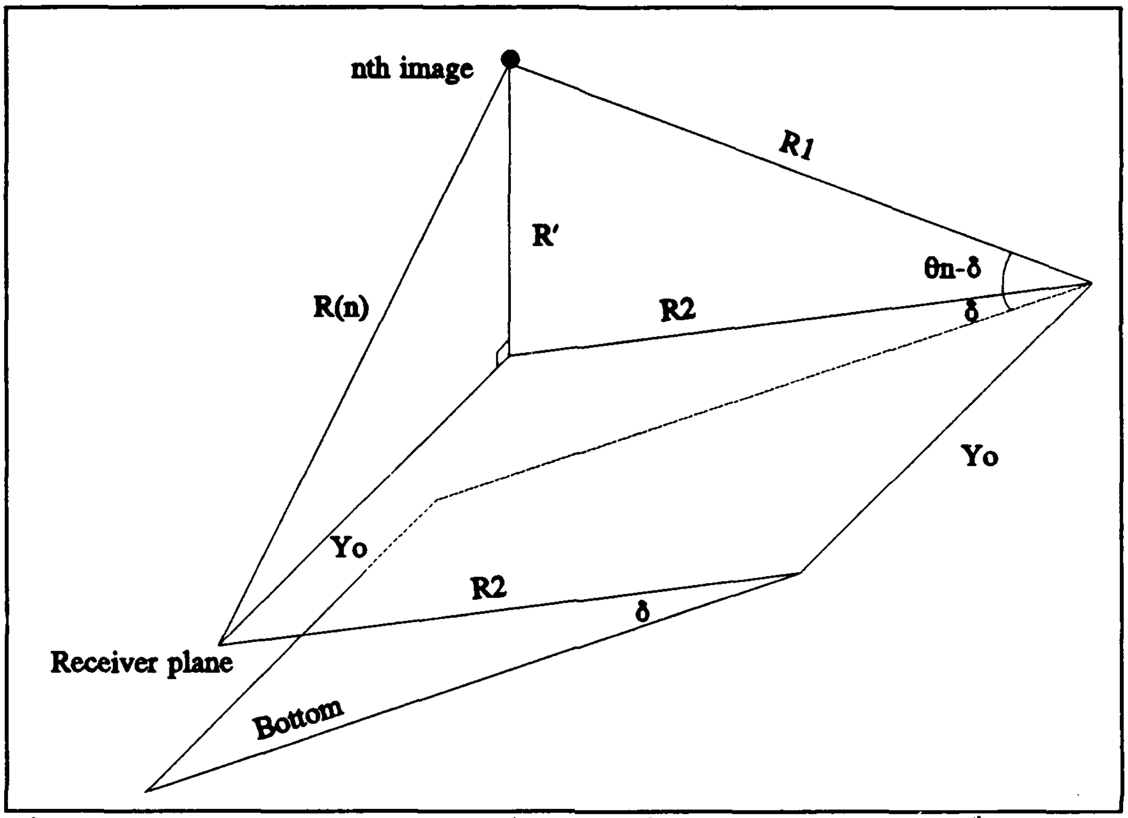

Figure 4. The Angle of Incidence θ_{nm} of the Upper n^{th} Image on the m^{th} Plane

The complex pressure from the upper images result in;

$$P_u = \sum_{n=1}^{N} \frac{1}{R(n)} \exp(-jkR(n))(-1)^{INT\,[(n+1)/2]} \prod_{m=1}^{M} R(\theta_{nm})$$

Where

$$\begin{aligned} \prod R(\theta_{nm}) &= 1 \quad for \quad n = 1 \\ &= -1 \quad for \quad n = 2 \end{aligned}$$

and from the lower images

$$P_l=\sum_{n=1}^{N}\frac{1}{R'(n)}\exp\,(-jkR'(n))(-1)^{INT\,[(n+1)/2]}\prod_{m=0}^{M}R(\theta'_{nm})$$

The total complex acoustic pressure P is the sum of the P_u and P_l

$$P = P_u + P_l$$

III. EVALUATION AND DISCUSSION

The effects of changing the source and receiver position on the prediction of the pressure field were evaluated at each reciprocal position.

The following fixed parameters were used,

β = 10°

D1 = 0.9

CC = 0.9

α/K_2 = 0.0183

The depictions of the pressure fields for these conditions as functions of R_1, R_2, γ, δ and Y_o are shown in figures. The specific data are shown in tables. The model was tested by varying either source or receiver and holding the other constant in each Y_o. The test was repeated after exchanging the positions of source and receiver. All the tests were done within ten normalized distances from apex.

A. ANGLE OF SOURCE, RECEIVER

The first case was examined by varying the angle with the source and receiver on axis-positions(Y_o=0). As depicted in Figure 5, there are two positions, one for source and another for receiver, and vise versa. The first position is set as constant R=10. The second position is set to R=1 at mid-depth

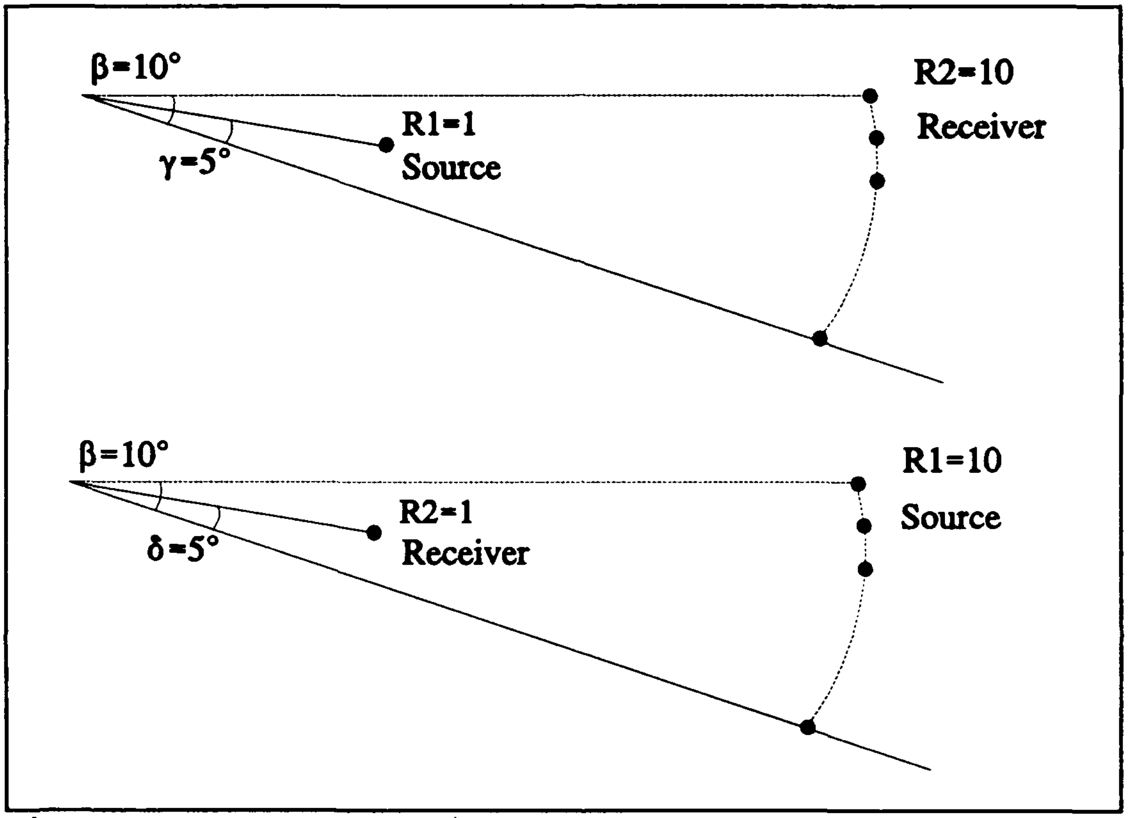

Figure 5. Geometry of Simple Tests

The depiction of the pressure field for these conditions as function of angle is shown in Figure 6. The corresponding overplot is shown in Figure 7, and Table 1 provides data of overall pressure.

Comparisons of pressure amplitudes at each reciprocal position shows that there are 1%-2.5% difference near the bottom (Figure 9 and 10), while they agree well near the surface (Figure 8) and at the middle depth. As the depth is deeper near the bottom,the ratio of difference to pressure ($\Delta P/P$) is larger. This pressure difference is probably the result of using the plane wave Rayleigh reflection coefficients, discussed by Kinsler, Frey, Coppens and Sanders[Ref. 10], when is only a good approximation if the sound source is not too close to the bottom.

B. DISTANCE FROM APEX

In this case, the distance from apex was varied with $Y_o=0$ and the same angular plane. One position is set as constant $R=10$ and another is varying from apex to $R=1$. The consistency of the pressure amplitude at each reciprocal position for various distance from apex is good near the surface and the mid-depth. But there are some pressure differences near the bottom. The overplot and data for this case are provided by Figure 11 and 12, Table 4.

As the distance from apex decreased, the ratio of difference to pressure ($\Delta P/P$) increased.

C. SHORE DISTANCE AS A VARIABLE

Until now, all studies were for on axis position ($Y_o=0$). In the following discussion the shore distance (Y_o) is the variable. All the above cases were re-examined with $Y_o=5$ and $Y_o=10$.

The graphs shown in Figure 13 through Figure 18 indicate the results of $Y_o = 5$ with a solid line and $Y_o = 10$ with the symbol connected by dashes. All the specific data were provided by Table 5 through 7. The pressure difference (ΔP) and the ratio of difference to pressure ($\Delta P/P$) near the surface for various angles were shown in Figures 13 and 14.

The results (Figures 15 and 16) show the ratio of difference to pressure ($\Delta P/P$) still shows decreasing error as source or receiver move away the bottom and increases with increasing Y_o.

Figures 17 and 18 show that as either the source or receiver approaches the apex, the ratio of difference to pressure($\Delta P/P$) becomes very high.

IV. CONCLUSION

A computer program used was created to predict the pressure of a point source everywhere within a wedge-shaped fluid overlying a fast bottom using the image method. This thesis was an attempt to compare the pressure amplitude for various reciprocal positions of source and receiver and to evaluate the validity of the image model in these conditions.

Figure 19 and 20 show the overplot of results for various configuration. Each graph indicates the overplot of pressure at reciprocal positions between source and receiver. $Y_o=0$ is indicated by a solid line, $Y_o=5$ with the dashes and $Y_o=10$ with the symbol connected by dashes.

Comparisons of pressure amplitude within the wedge at $Y_o=0$, 5, 10 for various angles are shown in Figure 19. Comparisons of pressure amplitude at mid-depth for various distances from the apex are shown in Figure 20. These comparisons show good consistency in each case.

The pressure amplitudes are more consistent at reciprocal positions when the position is near the surface and at mid-depth. The ratio of difference to pressure increases as the bottom is approached. This difference is probably caused by the failure of the plan-wave reflection coefficient when the source or receiver is near the bottom.

In the case of near the bottom, the distance from apex affects the consistency of the pressure, except for near the surface and mid-depth cases. As the distance from the apex increases, the ratio of difference to pressure ($\Delta P/P$) decreases. The ratio of difference to pressure ($\Delta P/P$) is also proportional to the shore distance in near the bottom case.

From the above results, it is concluded that the image model is valid for predicting the pressure in the sound field in a wedge-shaped layer overlying a fast penetrable bottom, except very close to the bottom and apex.

APPENDIX A: TABLES

Table 1. PRESSURE WITHIN WEDGE FOR VARIOUS ANGLES (Y_0 = 0)

γ	P	Constant	δ	P	Relative
0.0	0.04913	$R_1 = 10$	0.0	0.04795	$R_1 = 1$
1.0	0.16694	$R_2 = 1$	1.0	0.16561	$R_2 = 10$
2.0	0.25990	$\delta = 5°$	2.0	0.25882	$\gamma = 5°$
3.0	0.31425	$Y_0 = 0$	3.0	0.31365	$Y_0 = 0$
4.0	0.32956		4.0	0.32930	
5.0	0.31508		5.0	0.31501	
6.0	0.27836		6.0	0.27841	
7.0	0.22428		7.0	0.22442	
8.0	0.15702		8.0	0.15724	
9.0	0.08078		9.0	0.08108	
10.0	0.00000		10.0	0.00050	

Table 2. PRESSURE NEAR SURFACE FOR VARIOUS ANGLES (Y_0 = 0)

γ	P	Constant	δ	P	Relative
9.0	0.08078	$R_1 = 10$	9.0	0.08109	$R_1 = 1$
9.1	0.07283	$R_2 = 1$	9.1	0.07315	$R_2 = 10$
9.2	0.06484	$\delta = 5°$	9.2	0.06517	$\gamma = 5°$
0.3	0.05682	$Y_0 = 0$	9.3	0.05715	$Y_0 = 0$
9.4	0.04876		9.4	0.04910	
9.5	0.04068		9.5	0.04103	
9.6	0.03257		9.6	0.03293	
9.7	0.02444		9.7	0.02481	
9.8	0.01630		9.8	0.01668	
9.9	0.00815		9.9	0.00854	
10.0	0.00000		10.0	0.00050	

Table 3. PRESSURE NEAR BOTTOM FOR VARIOUS ANGLES (Y_0 = 0)

γ	P	Constant	δ	P	Relative	DEG	ΔP	$\Delta P/P$
0.0	0.04913	$R_1 = 10$	0.0	0.04795	$R_1 = 1$	0.0	0.00118	0.02402
0.1	0.06151	$R_2 = 1$	0.1	0.06029	$R_2 = 10$	0.1	0.00122	0.01983
0.2	0.07381	$\delta = 5°$	0.2	0.07256	$\gamma = 5°$	0.2	0.00125	0.01693
0.3	0.08601	$Y_0 = 0$	0.3	0.08474	$Y_0 = 0$	0.3	0.00127	0.01477
0.4	0.09809		0.4	0.09680		0.4	0.00129	0.01315
0.5	0.11002		0.5	0.10872		0.5	0.00130	0.01182
0.6	0.12180		0.6	0.12049		0.6	0.00131	0.01076
0.7	0.13340		0.7	0.13207		0.7	0.00133	0.00997
0.8	0.14480		0.8	0.14347		0.8	0.00133	0.00919
0.9	0.15598		0.9	0.15465		0.9	0.00133	0.00853
1.0	0.16694		1.0	0.16561		1.0	0.00133	0.00797

Table 4. PRESSURE NEAR BOTTOM FOR VARIOUS DISTANCES (Y_0 = 0)

R_1	P	Constant	R_2	P	Relative	R	ΔP	$\Delta P/P$
0.0	0.00000	$\gamma = 0.2°$	0.0	0.00003	$\gamma = 0.2°$	0.0	0.00003	1.00000
0.1	0.00067	$\delta = 0.2°$	0.1	0.00070	$\delta = 0.2°$	0.1	0.00003	0.04286
0.2	0.00238	$R_2 = 10$	0.2	0.00278	$R_1 = 10$	0.2	0.00040	0.14388
0.3	0.00815	$Y_0 = 0$	0.3	0.00891	$Y_0 = 0$	0.3	0.00076	0.08530
0.4	0.01967		0.4	0.02081		0.4	0.00114	0.05478
0.5	0.03616		0.5	0.03761		0.5	0.00145	0.03855
0.6	0.05328		0.6	0.05486		0.6	0.00158	0.02880
0.7	0.06713		0.7	0.06867		0.7	0.00154	0.02243
0.8	0.07670		0.8	0.07813		0.8	0.00143	0.01830
0.9	0.08246		0.9	0.08373		0.9	0.00127	0.01517
1.0	0.08548		1.0	0.08659		1.0	0.00111	0.01282

Table 5. PRESSURE DIFFERENCE, RATIO OF DIFFERENCE TO PRESSURE NEAR SURFACE FOR VARIOUS ANGLES (Y_0 = 5, Y_0 = 10)

DEG	ΔP	ΔP/P	Constant	ΔP	ΔP/P	Relative
9.0	0.00042	0.00552	$R_{1,2}$=1,10	0.00067	0.00875	$R_{1,2}$=1,10
9.1	0.00043	0.00626	$\gamma = 5°$	0.00070	0.01011	$\gamma = 5°$
9.2	0.00043	0.00703	$\delta = 5°$	0.00074	0.01197	$\delta = 5°$
9.3	0.00044	0.00821	$Y_0 = 5$	0.00078	0.01435	$Y_0 = 10$
9.4	0.00044	0.00955		0.00081	0.01729	
9.5	0.00045	0.01169		0.00084	0.02138	
9.6	0.00046	0.01489		0.00088	0.02780	
9.7	0.00047	0.02116		0.00091	0.03789	
9.8	0.00048	0.03055		0.00094	0.05735	
9.9	0.00050	0.06158		0.00097	0.11162	
10.0	0.00075	1.00000		0.00105	1.00000	

Table 6. PRESSURE DIFFERENCE, RATIO OF DIFFERENCE TO PRESSURE NEAR BOTTOM FOR VARIOUS ANGLES (Y_0 =5, Y_0 =10)

DEG	ΔP	ΔP/P	Constant	ΔP	ΔP/P	Relative
0.0	0.00087	0.02148	$R_{1,2}$=1,10	0.00071	0.02536	$R_{1,2}$=1,10
0.1	0.00089	0.01780	$\gamma = 5°$	0.00072	0.02081	$\gamma = 5°$
0.2	0.00090	0.01515	$\delta = 5°$	0.00074	0.01797	$\delta = 5°$
0.3	0.00092	0.01338	$Y_0 = 5$	0.00076	0.01592	$Y_0 = 10$
0.4	0.00093	0.01191		0.00077	0.01419	
0.5	0.00095	0.01088		0.00080	0.01317	
0.6	0.00097	0.01006		0.00081	0.01206	
0.7	0.00098	0.00929		0.00082	0.01115	
0.8	0.00099	0.00866		0.00084	0.01052	
0.9	0.00100	0.00812		0.00085	0.00987	
1.0	0.00102	0.00774		0.00087	0.00942	

Table 7. **PRESSURE DIFFERENCE, RATIO OVER DIFFERENCE TWO PRESSURE NEAR BOTTOM FOR VARIOUS DISTANCES (Y_0 = 5, Y_0 = 10)**

R	ΔP	ΔP/P	Constant	ΔP	ΔP/P	Relative
0.0	0.00002	1.00000	$R_{1,2}$=1,10	0.00004	1.00000	$R_{1,2}$=1,10
0.1	0.00000	0.00000	$\gamma = 0.2°$	0.00013	0.08844	$\gamma = 0.2°$
0.2	0.00013	0.05603	$\delta = 0.2°$	0.00023	0.07395	$\delta = 0.2°$
0.3	0.00043	0.07963	$Y_0 = 5$	0.00036	0.06679	$Y_0 = 10$
0.4	0.00077	0.06190		0.00055	0.06180	
0.5	0.00105	0.04370		0.00081	0.05625	
0.6	0.00121	0.03176		0.00105	0.04719	
0.7	0.00123	0.02404		0.00119	0.03781	
0.8	0.00117	0.01907		0.00118	0.02932	
0.9	0.00108	0.01577		0.00109	0.02316	
1.0	0.00097	0.01328		0.00097	0.01868	

APPENDIX B: FIGURES

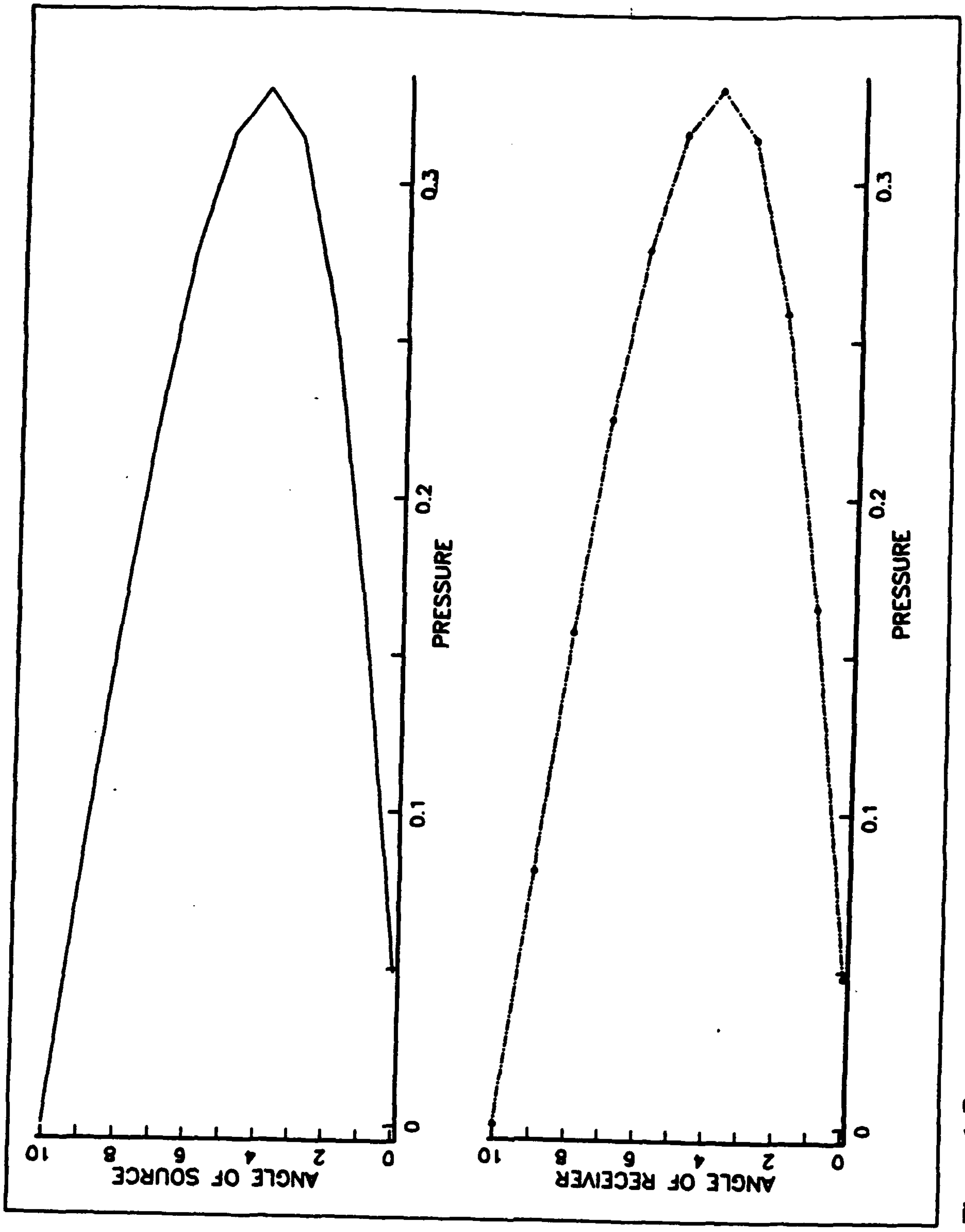

Figure 6. Pressure Amplitude within Wedge at Y_0 for Various Angle
(a) Various Source Angles, (b) Various Receiver Angles

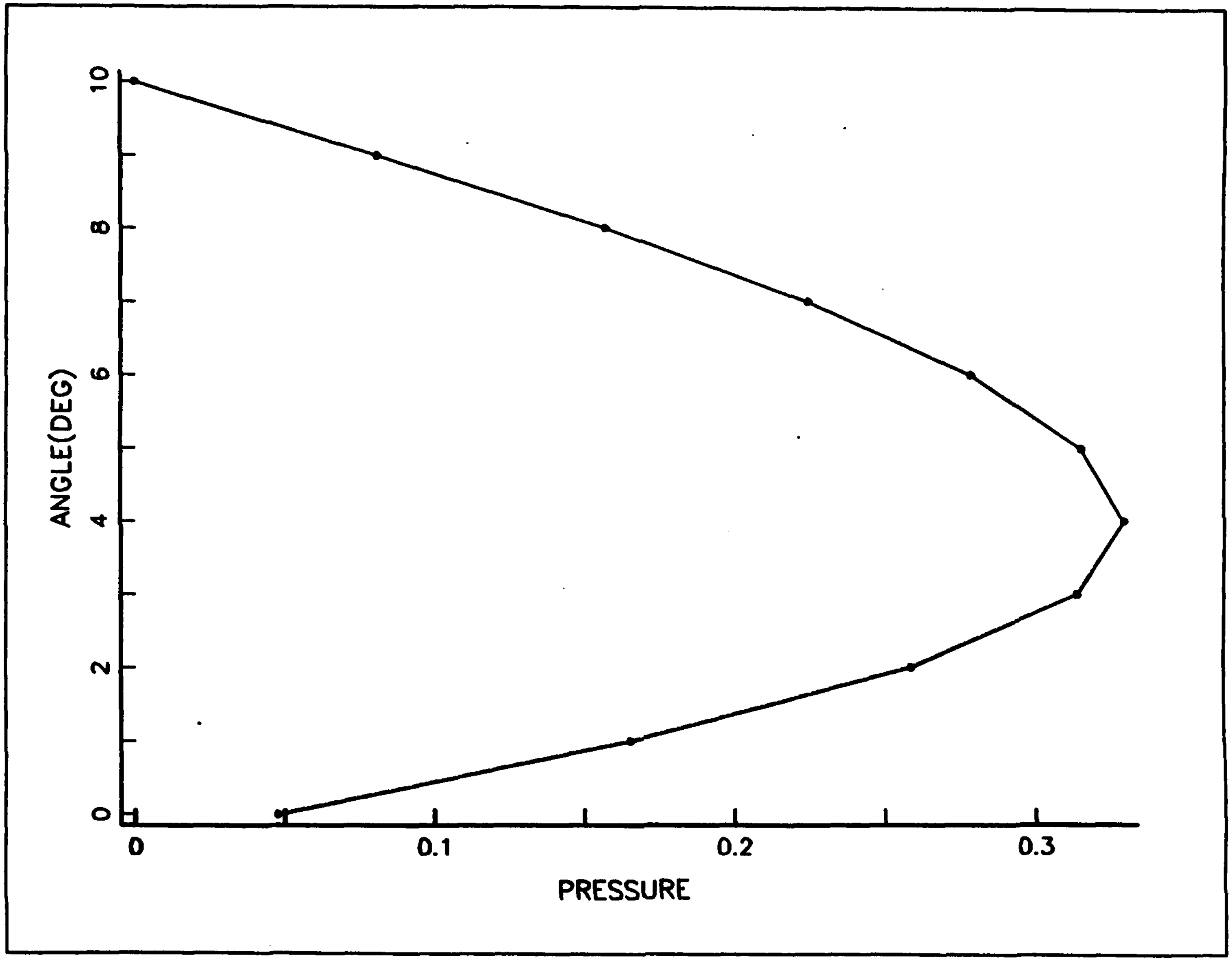

Figure 7. Overplot of Fig.6(a) and 6(b)

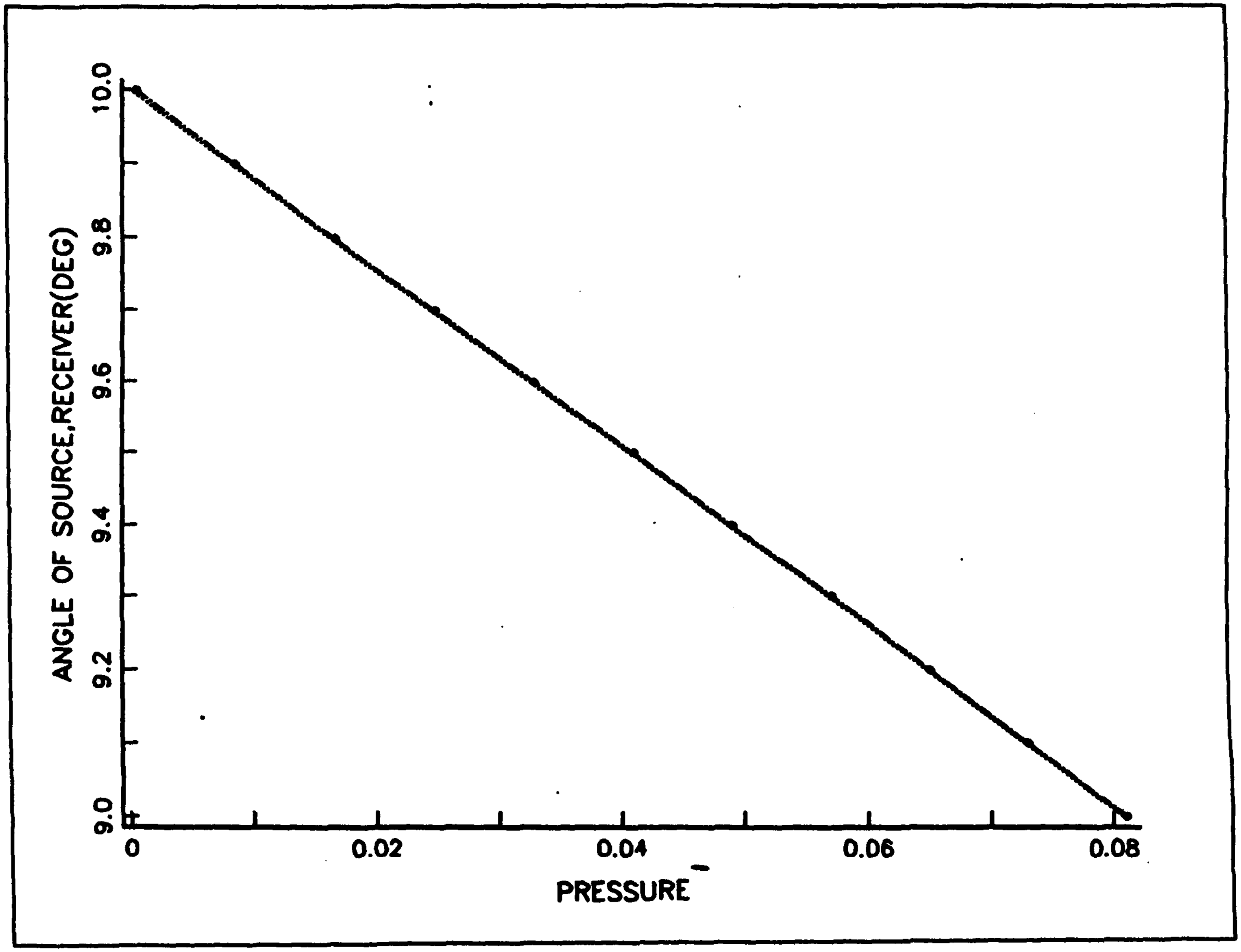

Figure 8. Overplot of Pressure in the Reciprocal Position Near the Surface at $Y_e = 0$ for Various Angles

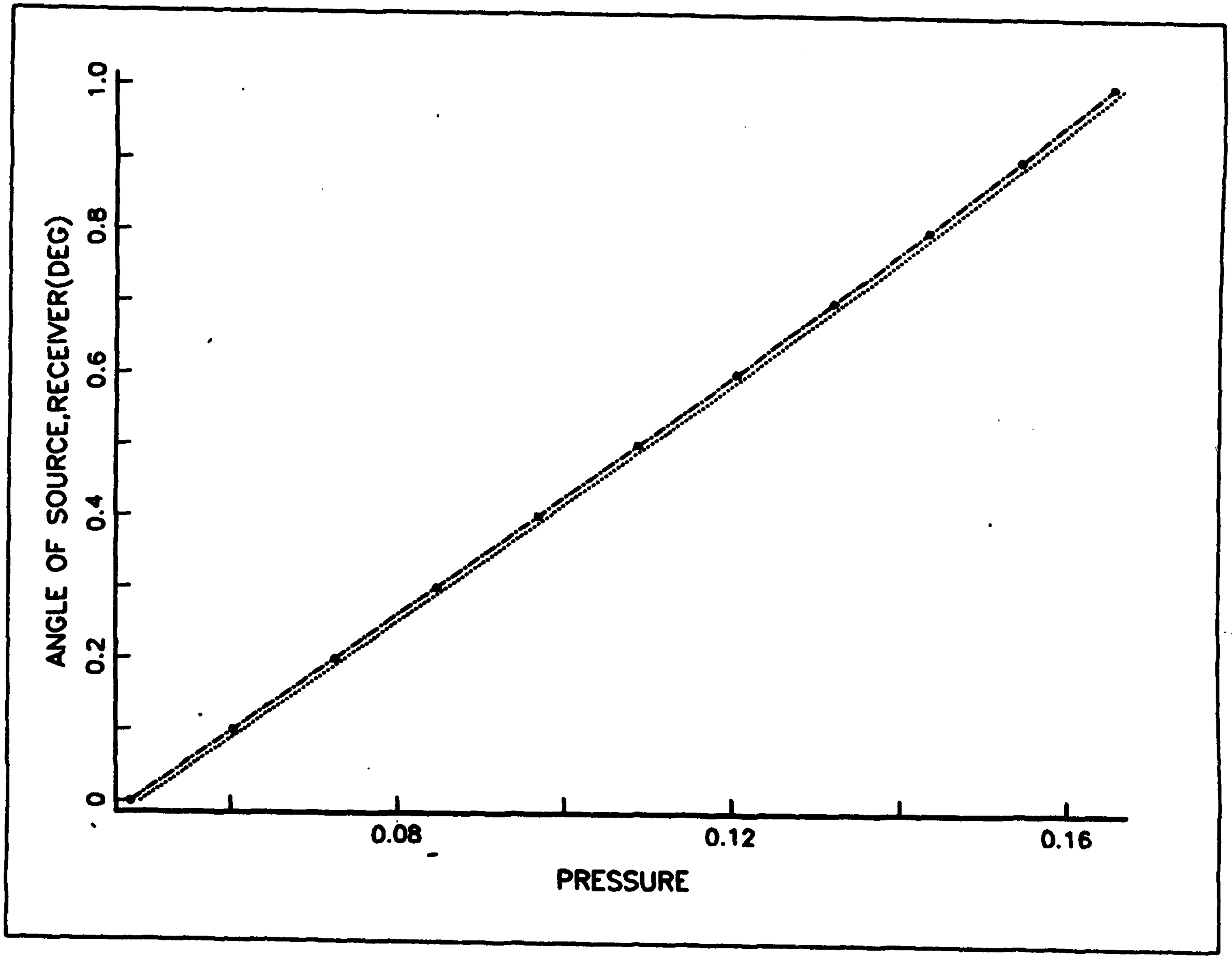

Figure 9. Overplot of Pressure in the Reciprocal Position Near the Bottom at $Y_s=0$ for Various Angles

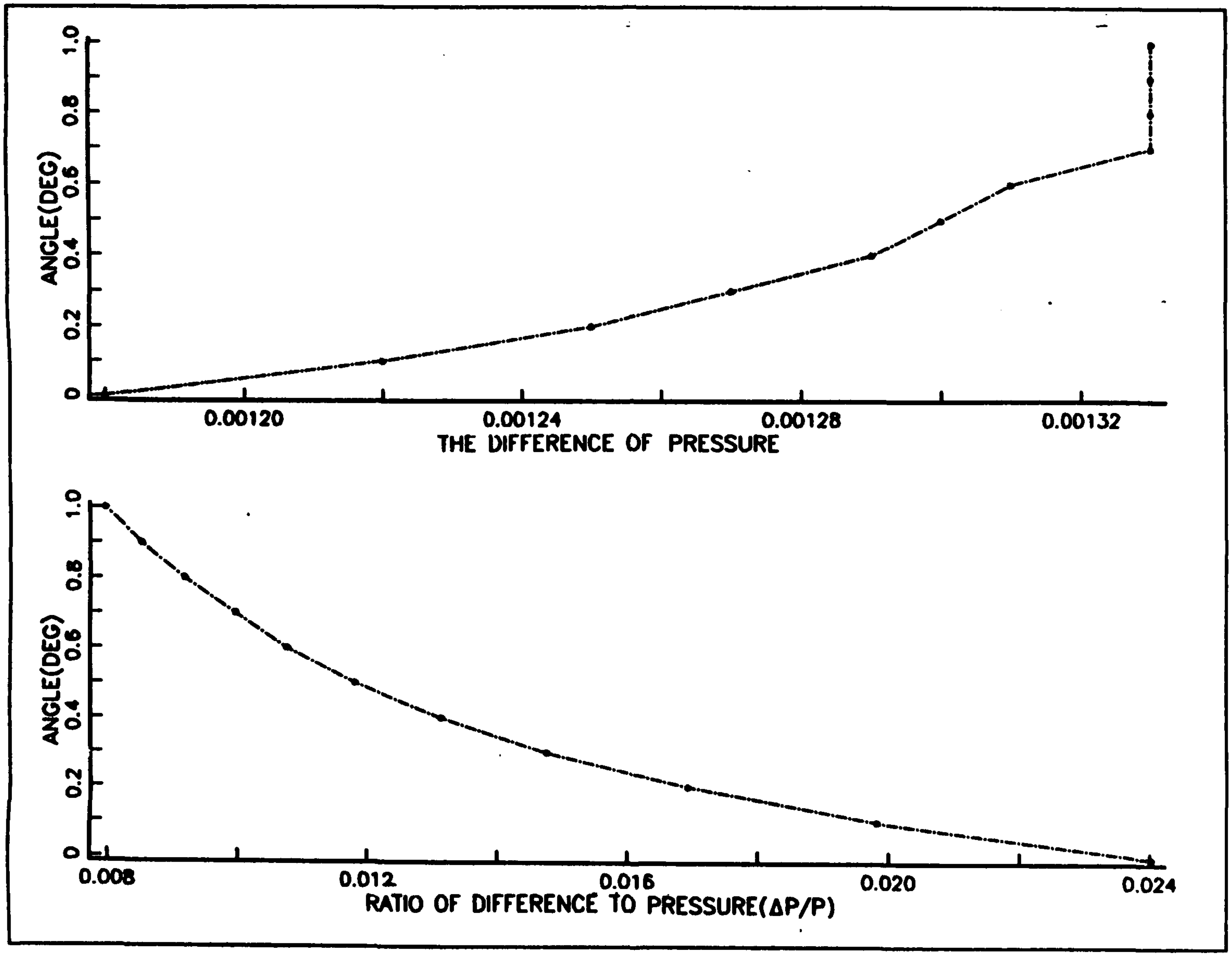

Figure 10. Pressure Difference(ΔP) and Ratio of Difference to Pressure(ΔP/P) for Fig.9

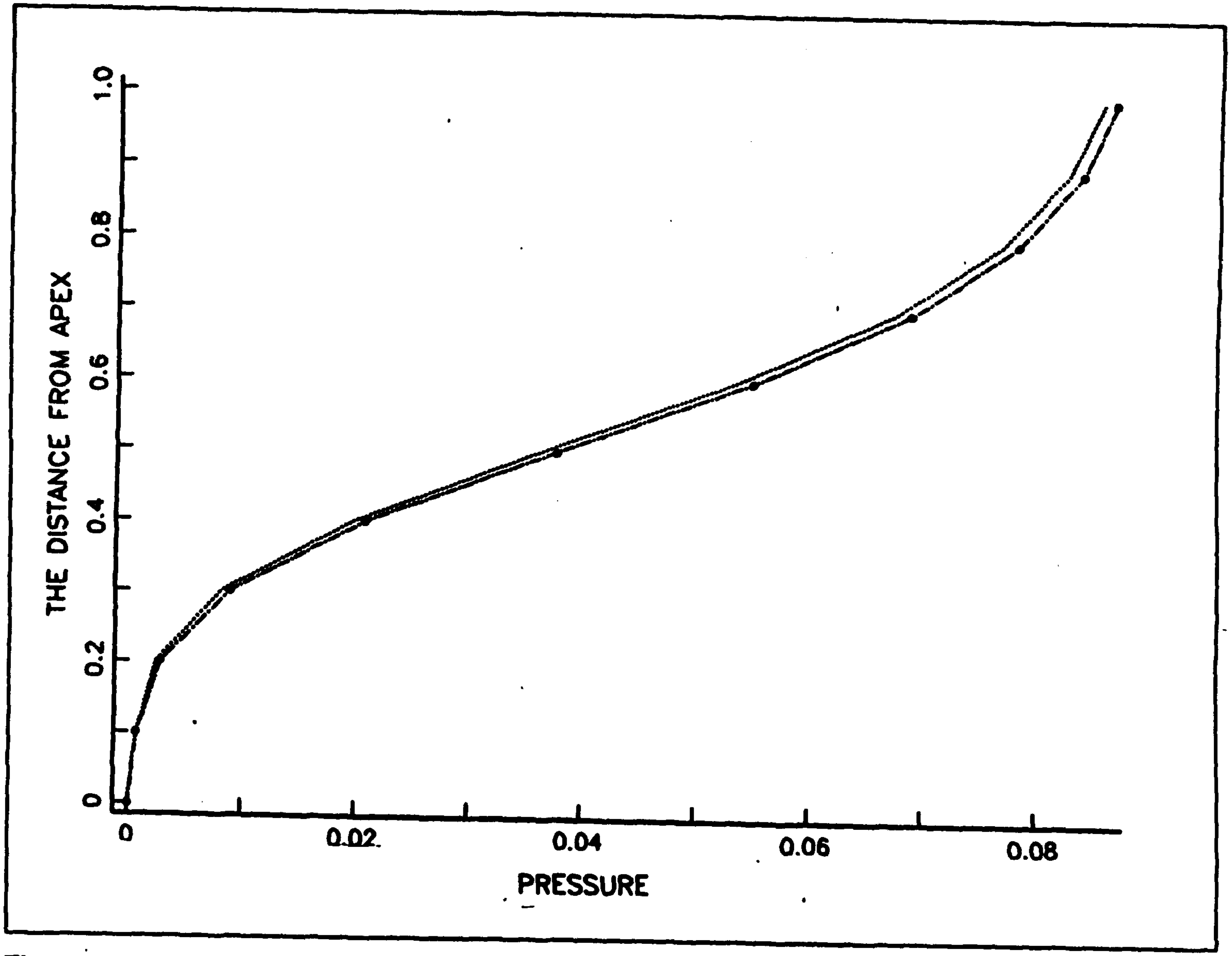

Figure 11. Overplot of Pressure in the Reciprocal Position Near the Bottom at $Y_e=0$ for Various Distance from Apex

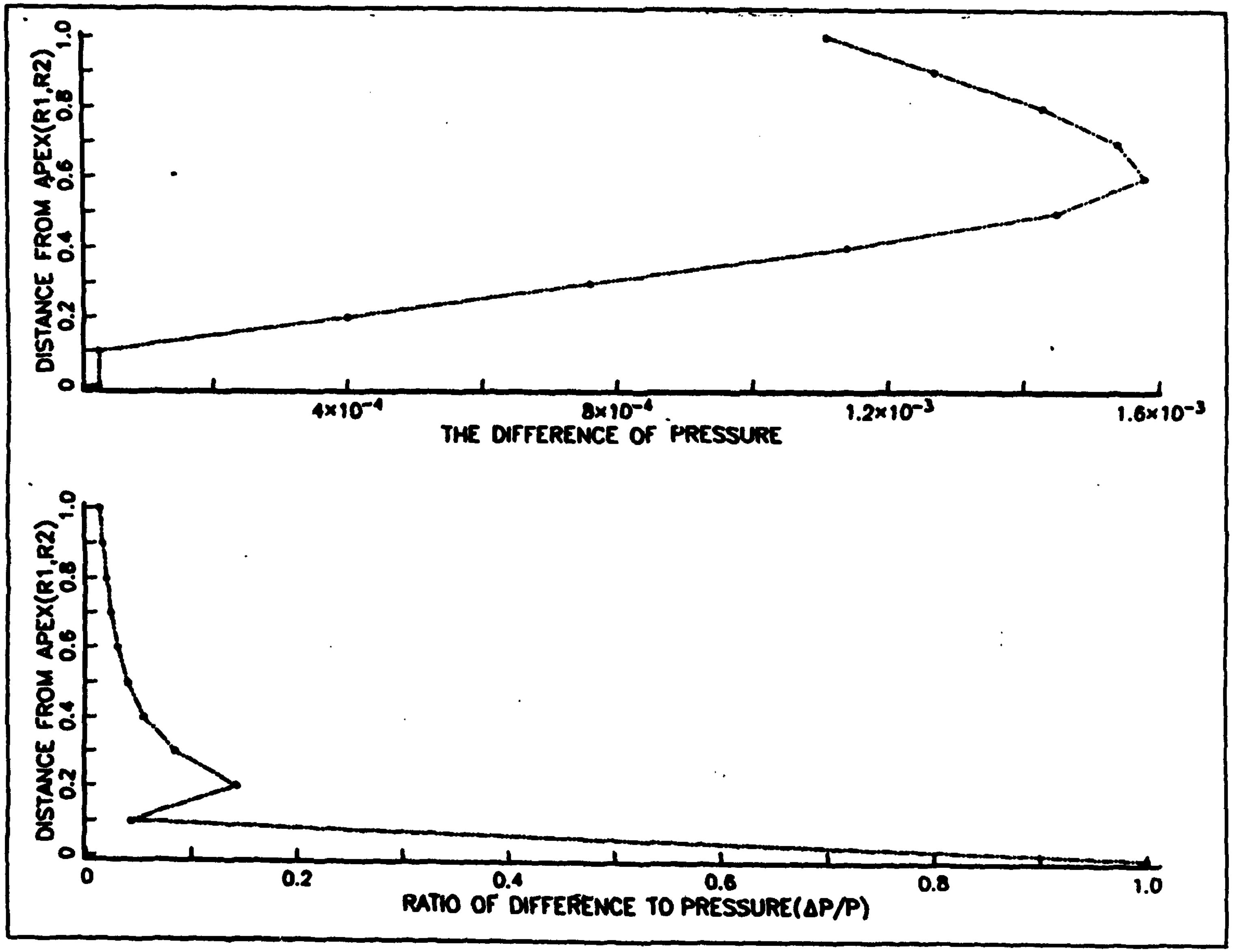

Figure 12. Pressure Difference(ΔP) and Ratio of Difference to Pressure($\Delta P/P$) for Fig.11

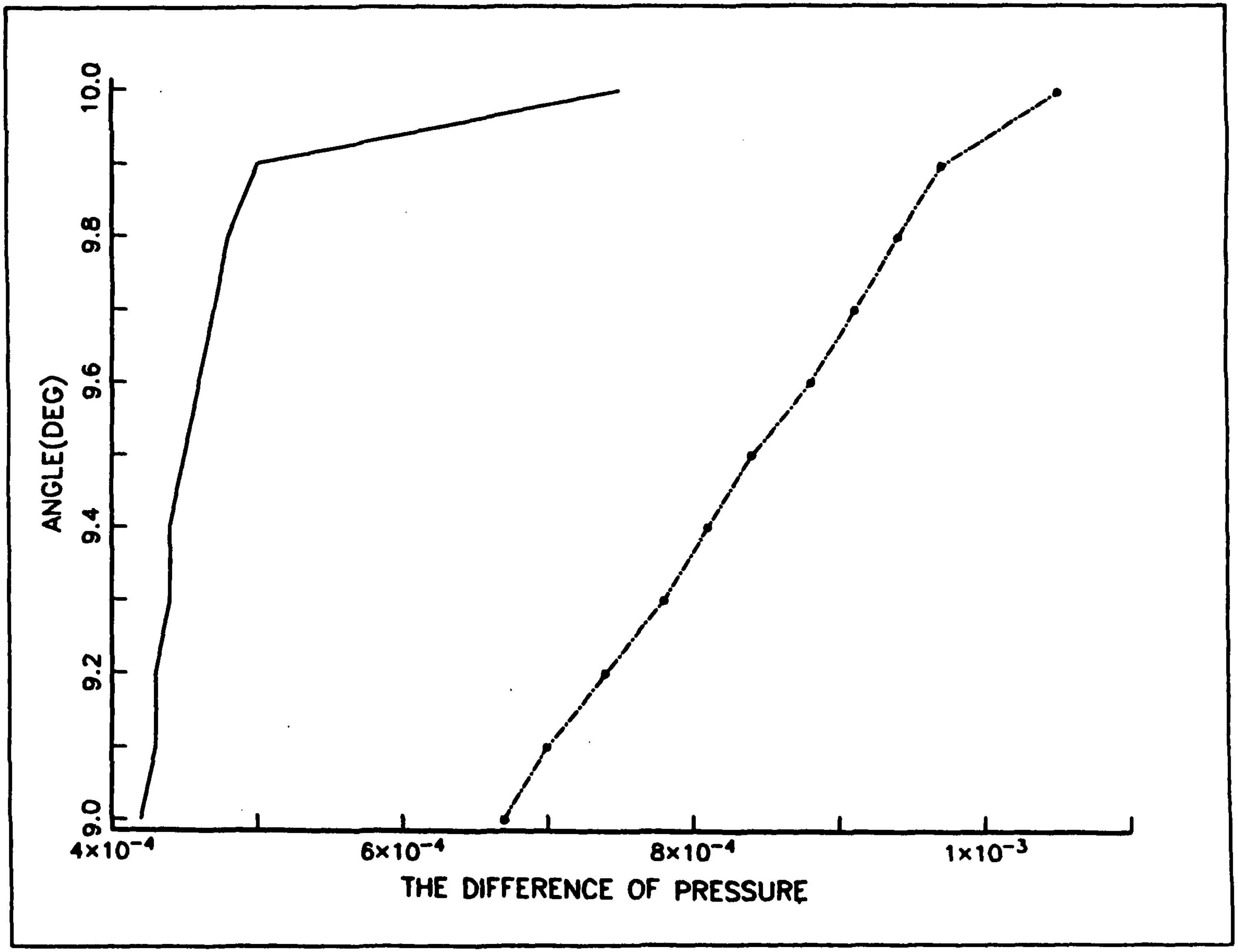

Figure 13. Pressure difference(ΔP) Near the Surface at $Y_{*}=5$, 10 for Various angles

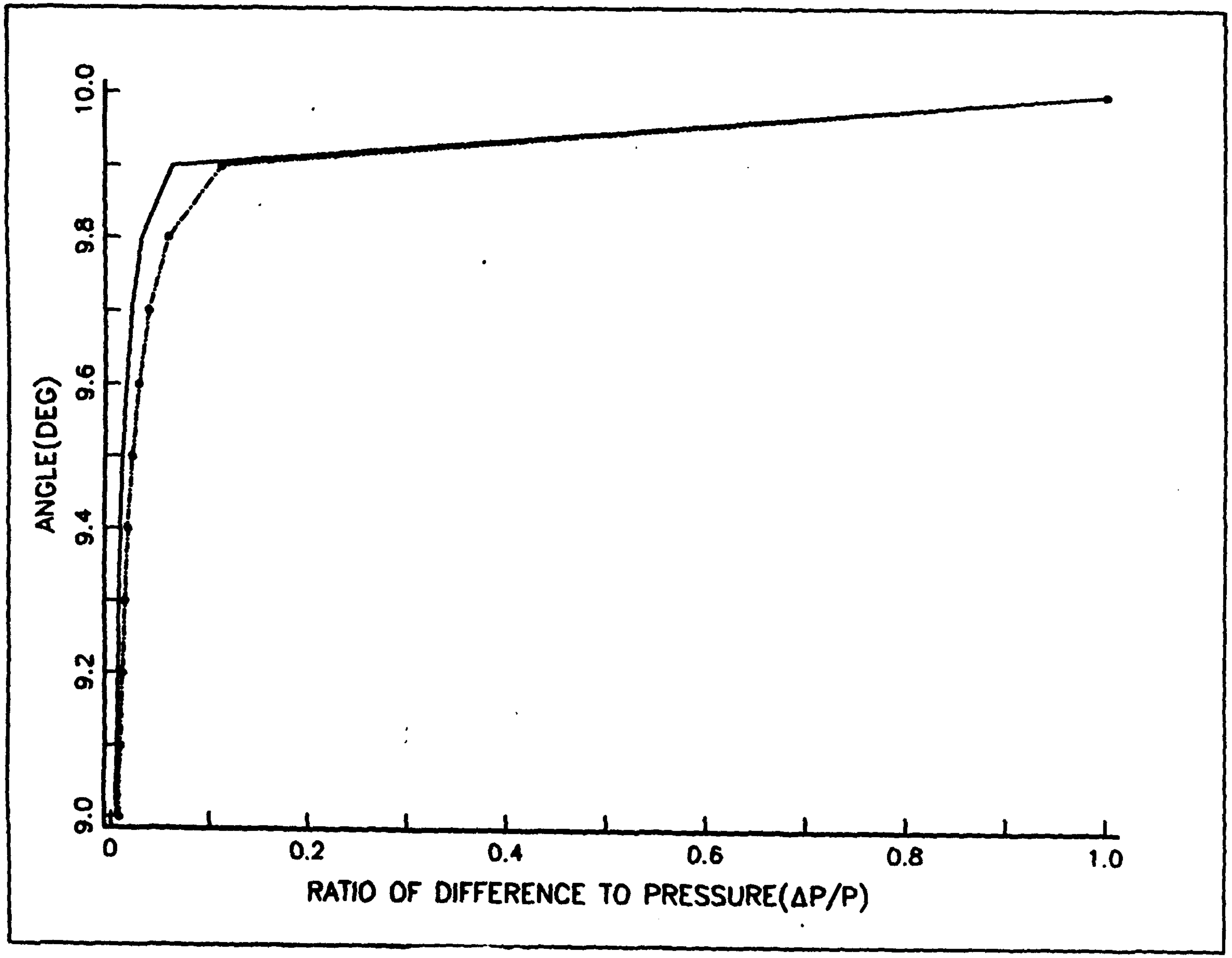

Figure 14. Ratio of Difference to Pressure(ΔP/P) Near the Surface at Y_o=5, 10 for Various Angles

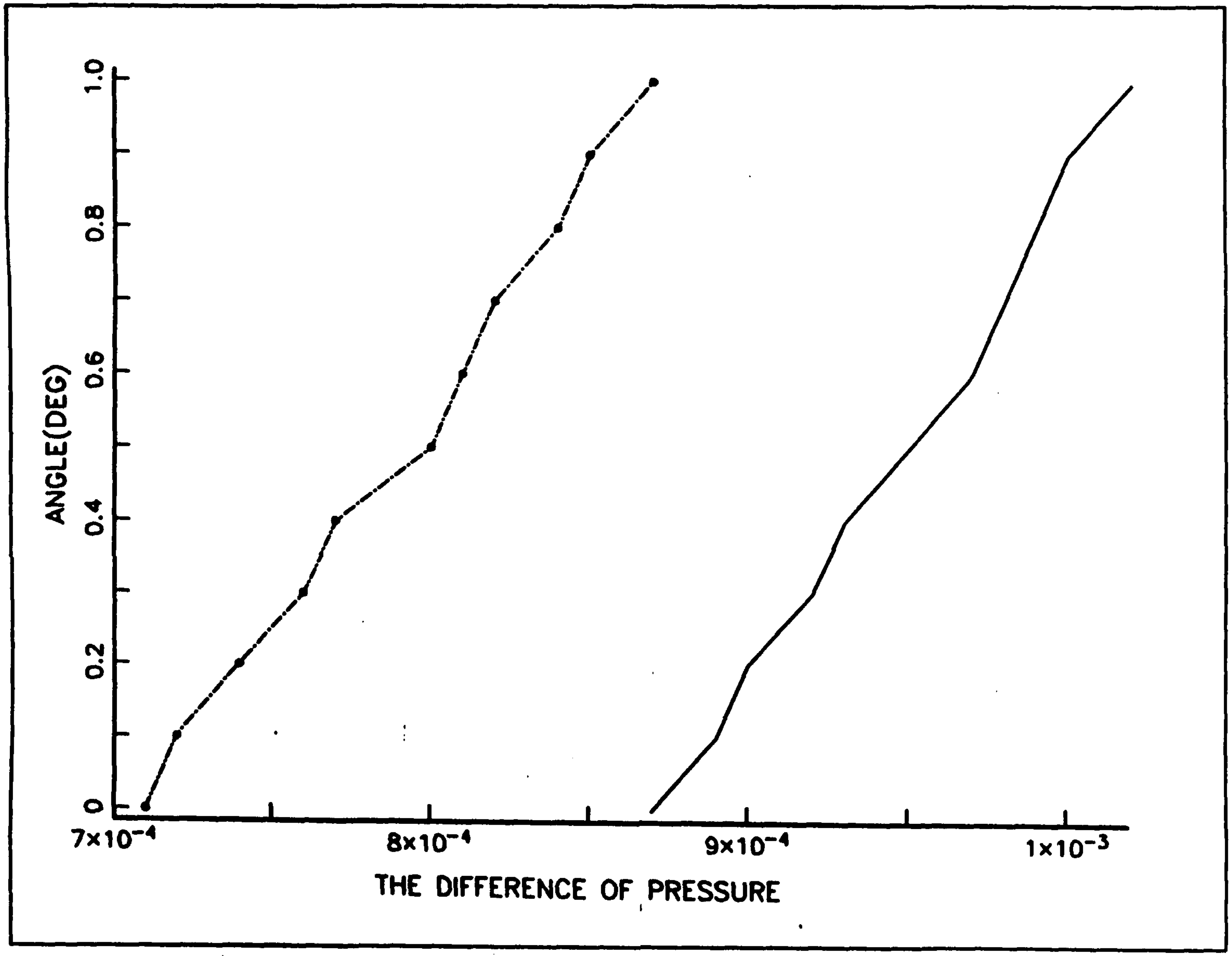

Figure 15. Pressure difference(ΔP) Near the Bottom at Y_o=5, 10 for Various angles

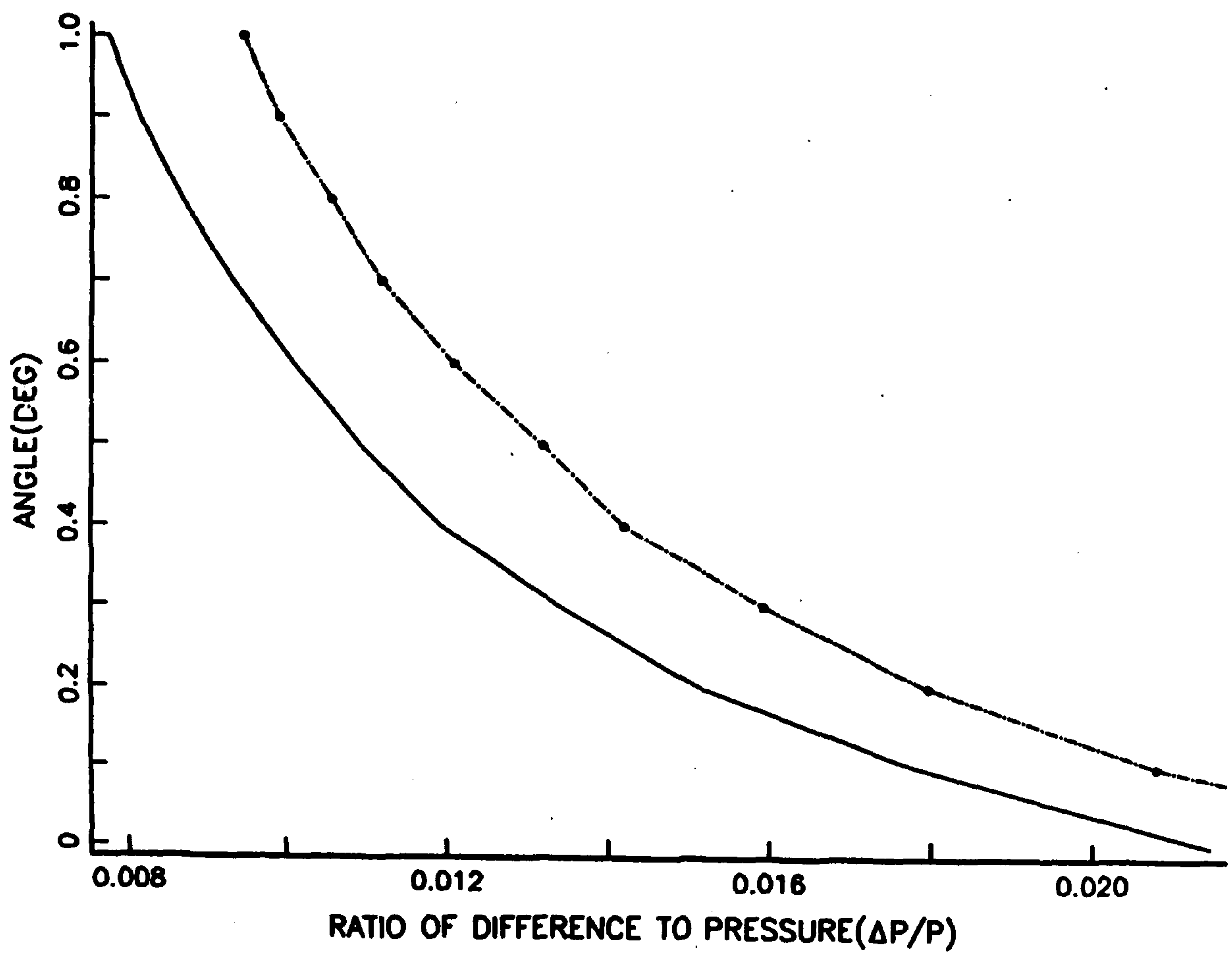

Figure 16. Ratio of Difference to Pressure($\Delta P/P$) Near the Bottom at $Y_{*}=5$, 10 for Various Angles

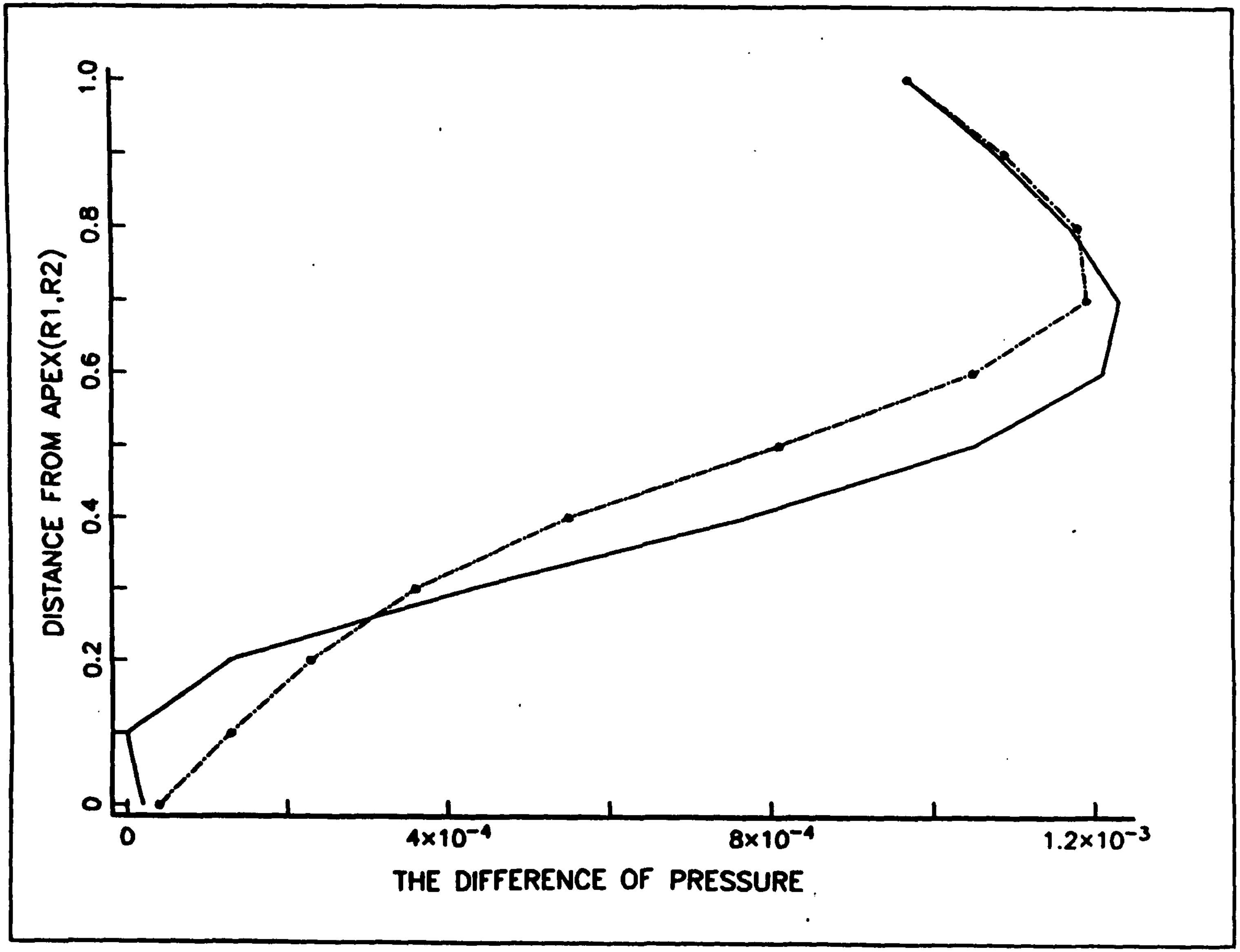

Figure 17. Pressure difference(ΔP) Near the Bottom at $Y_{*}=5$, 10 for Various Distances from Apex

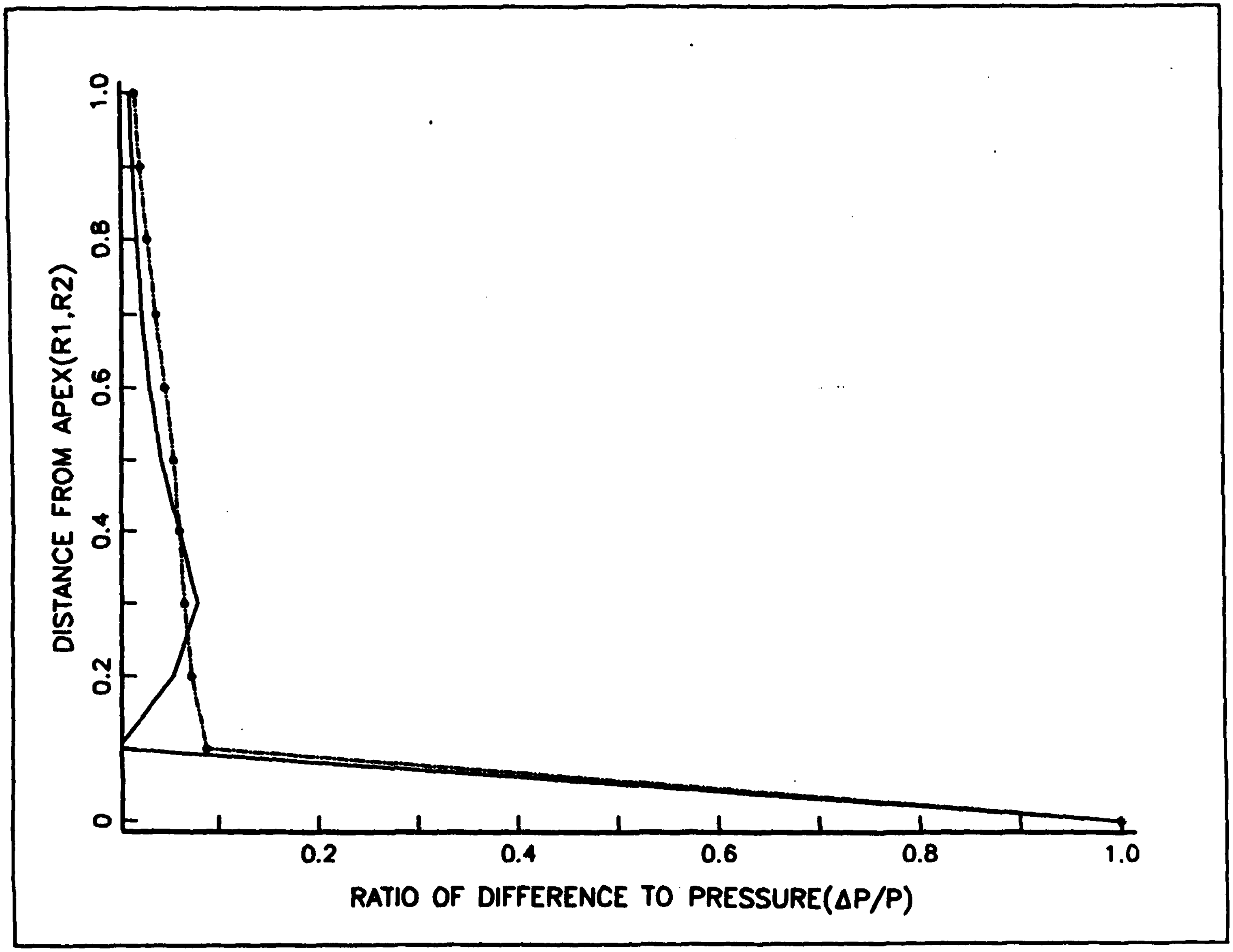

Figure 18. Pressure difference(ΔP) Near the Bottom at Y_o=5, 10 for Various Distances from Apex

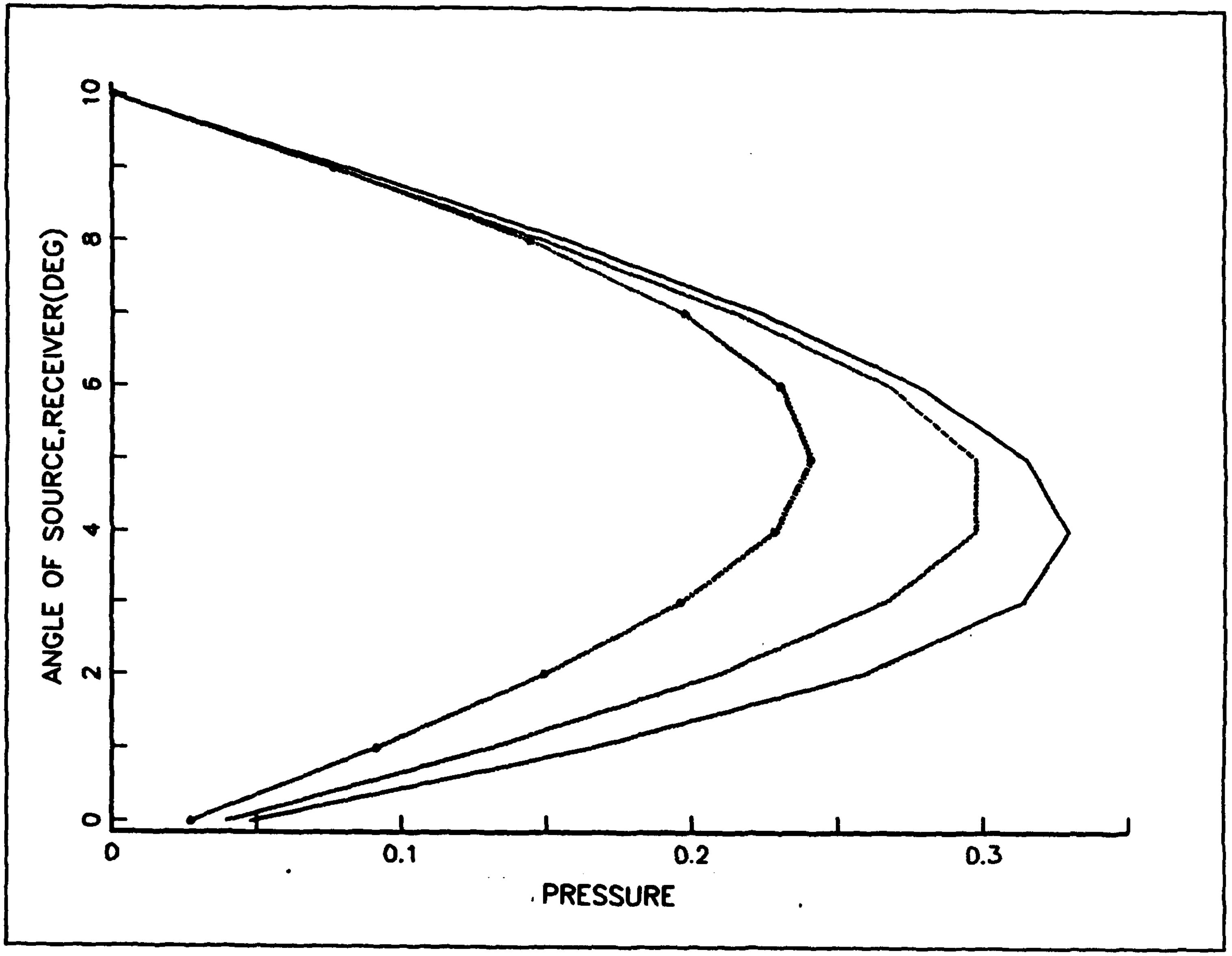

Figure 19. Overplot of Pressure Amplitude in the Reciprocal Position at $Y_e=0, 5, 10$ for Various angles

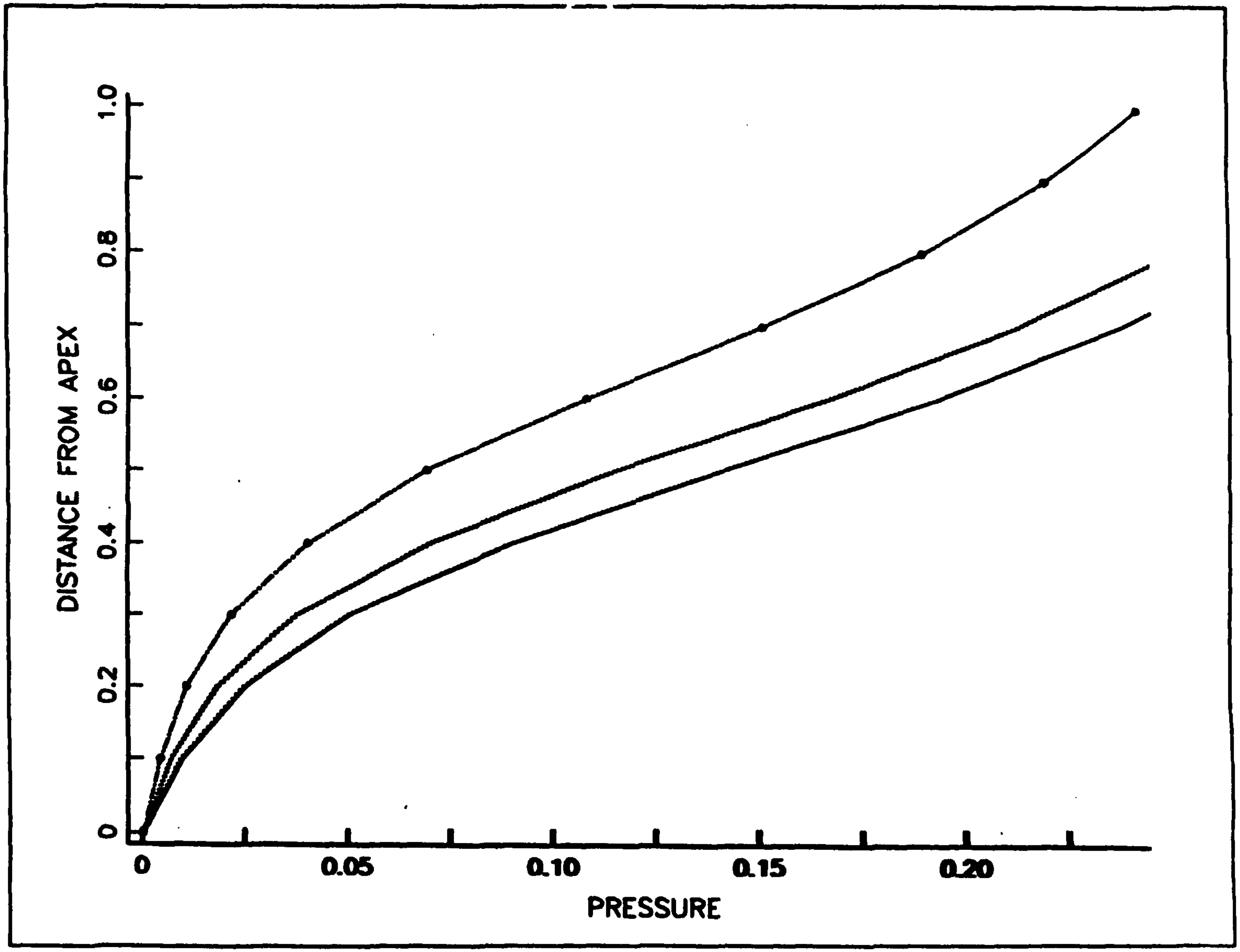

Figure 20. Overplot of Pressure Amplitude in the Reciprocal Position Near the Bottom at $Y_{*}=0, 5, 10$ for Various Distances from Apex

APPENDIX C: COMPUTER PROGRAM

```
**************************************************************************
* POPIMA
* IMAGE THEORY--CROSS SLOPE POINT FIELD PRESSURE
******************************
      INTEGER   I,I1,N,S1,S2,N1,K
      REAL*4    B,CC,C2,D,D1,D2,G,PI,P1,P2,Q1,R1,R2,T,
     *          T4,T6,W0,W1,Y0,Y1,Y2,Z1,Z2,Z3,Z4,Z5,Z6,
     *          T1(900),R8(900),R9(900),S(900),C(900),E(900),
     *          F(900),Y,Z,R3,AL,PZ(900)
      REAL  TQQ,TQQ1,TQQ2,TQQ3
      PI =ACOS(-1.0D00)
      WRITE(*,*)'INPUT B,G,D1,CC,R1,R2,AL,Y0'
      READ(6,*)B,G,D1,CC,R1,R2,AL,Y0

C     CALL EXCMS('FILEDEF 11 CLEAR')
      DATA NOO/11/
      DATA NOU/10/
      CALL EXCMS('FILEDEF 11 DISK POP6 PLOTTER A1')
      CALL EXCMS('FILEDEF 10 DISK POP6 DATA A1')
        D=-0.1
        K=0
      DO 20  M =0,10
        D=D+0.1
        K=K+1
      WRITE(NOU,2) B,G,D,D1,CC,R1,R2,AL,Y0
    2 FORMAT(3X,'B = ',F4.1,/,3X,'G = ',F4.1,/,3X,'D = ',F4.1,/,3X,'D1 =
     * ',F4.1,/,3X,'CC = ',F4.1,/,3X,'R1 = ',F4.1,/,3X,'R2 = ',F4.1,/,3X
     *,'AL = ',F6.3 ,/,3X,'YO = ',F4.1)

C*********************************************************************
C     INPUT PARAMETERS
C*********************************************************************
C     B = WEDGE ANGLE (DEG) = 180/N1
```

```
C    G = SOURCE ANGLE (DEG)
C    D = RECEIVER ANGLE (DEG)
C    N1= # OF IMAGE POINTS
C    R1 = SOURCE DISTANCE (IN DUMP DISTANCES) FROM APEX
C    R2 = RECEIVER DISTANCE (IN DUMP DISTANCES) FROM APEX
C    Y0 = DISTANCE (IN DUMP DISTANCES) ALONG APEX
C    D1 = RHO1/RHO2
C    CC = C1/C2
C    AL = ALPHA/K2
C    A  = # OF RECEIVER POSITIONS
C    D = 5.0
C ]------------------------------------------]
C ]CHOOSE SLOW OR FAST BOTTOM BY VALUE OF SPEED RATIO  ]
C ]CC = C1/C2 .                                 ]
C ]------------------------------------------]
C*************************************************************************
C                    MAIN PROGRAM
C*************************************************************************
     N1 = INT(180./B)
     T6 = 180./PI
     B  = B/T6
     G  = G/T6
     D  = D/T6
     C2 = CC**2
     TQQ = TAN(B)
C ------------------------------------------------
C DECISION ABOUT SLOW OR FAST BOTTOM
C    T4 = PI/(2*SIN(ACOS(CC))*TAN(B)) FOR FAST BOTTOM
C    T4 = PI/(2*TAN(ACOS(1/CC))*TAN(B)) FOR SLOW BOTTOM
C ------------------------------------------------
C
     IF (CC.LT.1) THEN
       TQQ1 =ACOS(CC)
       TQQ2 = SIN(TQQ1)
     ELSE
       TQQ1 = ACOS(1/CC)
       TQQ2 = TAN(TQQ1)
```

```
      ENDIF
      TQQ3 = 2.*TQQ2*TQQ
      T4   = PI/TQQ3
      Q1   = 1/DSQRT(2.0D00)
         D2 = (Y0*Y0)+(R1*R1)+(R2*R2)
         R3 = 2.*R1*R2
         S1 = 1
C     |-----------------------------------|
C     |THIS DO LOOP CALCULATES THE THETA(N)      |
C     |AND THE IMAGE SLANT RANGES R8(N) AND R9(N)|
C     |-----------------------------------|
         DO 30  N = 1, N1
           IF(S1.GT.0) T1(N) = (N-1)*B+G
           IF(S1.LT.0) T1(N) = N*B-G
           S1 = - S1
           R8(N) = SQRT(D2-R3*COS(T1(N)-D))
           R9(N) = SQRT(D2-R3*COS(T1(N)+D))
 30       CONTINUE
C      |--------------------------|
C      |SUM THE PRESSURE OVER ALL IMAGES|
C      |--------------------------|
         P1 = 0.0
         P2 = 0.0
         DO 40  N = 1, N1
           S2 = (-1)**(INT(N/2))
C      |-----------------------------------|
C      |REFLECTION COEFFICIENTS ALONG NTH UPPER PATH|
C      |-----------------------------------|
           W1 = 2*C2*AL
           I1 = INT((N-1)/2)
           DO 50  I = 1,I1
             S(I) = ABS(R1*SIN(T1(N)-2*I*B)
     &                        +R2*SIN(2*I*B-D))/R8(N)
             IF(S(I).GE.1) S(I)=1
             C(I) = SQRT(1-(S(I)*S(I)))
             T  = S(I)/D1
             W0 = (-C2+(C(I)*C(I)))
```

```
      Y  = SQRT((W0*W0)+(W1*W1))
      Z  = ABS(W0)
      IF(Y.LE.Z) Y = Z
      Y1 =  Q1*SQRT(Y+W0)
      Y2 = -Q1*SQRT(Y-W0)
      Z1 =  T-Y2
      Z2 = -Y1
      Z3 =  Z1/(Z1*Z1+Z2*Z2)
      Z4 = -Z2/(Z1*Z1+Z2*Z2)
      Z1 =  T+Y2
      Z2 =  Y1
      Z5 =  Z1*Z3-Z2*Z4
      Z6 = Z1*Z4+Z2*Z3
      E(I) = Z5
      F(I) = Z6
 50   CONTINUE
C    |-----------------------------------------------|
C    |PRODUCT OF REFLECTION COEFFICIENTS ALONG NTH UPPER PATH|
C    |-----------------------------------------------|
      Z1 = 0
      Z2 = 0
      Z3 = 0
      Z4 = 0
      Z5 = 1
      Z6 = 0
      IF(N.LE.2.00) GOTO 110
      DO 60  I = 1, I1
        Z1 = E(I)
        Z2 = F(I)
        Z3 = Z5
        Z4 = Z6
        Z5 = Z1*Z3-Z2*Z4
        Z6 = Z1*Z4+Z2*Z3
 60   CONTINUE
 110  Z1 = Z5
      Z2 = Z6
      T  = T4*R8(N)
```

```
      Z3 = COS(T)
      Z4 = -SIN(T)
      Z5 = Z1*Z3-Z2*Z4
      Z6 = Z1*Z4+Z2*Z3
      P1 = P1+S2*Z5/R8(N)
      P2 = P2+S2*Z6/R8(N)
C      WRITE(6,*) 'I=',I, ' P1=',P1,' P2=',P2
      I1=I1+1
C    |-------------------------------------|
C    |REFLECTION COEFFICIENTS ALONG NTH LOWER PATH|
C    |-------------------------------------|
      DO 70 I = 1, I1
        S(I) = ABS(R1*SIN(T1(N)-2*(I-1)*B)
     &                 + R2*SIN(2*(I-1)*B+D))/R9(N)
        IF(S(I).GT.1) S(I)=1
        C(I) = SQRT(1.001-S(I)*S(I))
        T = S(I)/D1
        W0 = -C2+C(I)*C(I)
        Y = SQRT((W0*W0)+(W1*W1))
        Z = ABS(W0)
        IF(Y.LE.Z) Y = Z
        Y1 = Q1*SQRT(Y+W0)
        Y2 = -Q1*SQRT(Y-W0)
        Z1 = T-Y2
        Z2 = -Y1
        Z3 = Z1/(Z1*Z1+Z2*Z2)
        Z4 = - Z2/(Z1*Z1+Z2*Z2)
        Z1 = T+Y2
        Z2 = Y1
        Z5 = Z1*Z3-Z2*Z4
        Z6 = Z1*Z4+Z2*Z3
        E(I)=Z5
        F(I)=Z6
 70   CONTINUE
```

```
C      |----------------------------------------------------|
C      |PRODUCT OF REFLECTION COEFFICIENTS ALONG NTH LOWER PATH|
C      |----------------------------------------------------|
          Z1 = 0
          Z2 = 0
          Z3 = 0
          Z4 = 0
          Z5 = 1
          Z6 = 0
          DO 80 I = 1,I1
            Z1 = E(I)
            Z2 = F(I)
            Z3 = Z5
            Z4 = Z6
            Z5 = Z1*Z3-Z2*Z4
            Z6 = Z1*Z4+Z2*Z3
 80         CONTINUE
          Z1 = Z5
          Z2 = Z6
          T  = T4*R9(N)
          Z3 = COS(T)
          Z4 = -SIN(T)
          Z5 = Z1*Z3-Z2*Z4
          Z6 = Z1*Z4+Z2*Z3
          P1 = P1+S2*Z5/R9(N)
          P2 = P2+S2*Z6/R9(N)
 40       CONTINUE
        PZ(K) = SQRT(P1*P1+P2*P2)
        WRITE(NOU,3) PZ(K)
 3     FORMAT(3X,'PZ = ',F9.5,/)
       B=B*T6
       G=G*T6
       D=D*T6
       WRITE(NOO,4) D,PZ(K)
 4     FORMAT(3X,F4.1,3X,F9.5)
 20    CONTINUE
       END
```

LIST OF REFERENCES

1. Bradley, D., and Hudimac, A.A., *The Propagation of Sound in a Wedge Shaped Shallow Water Duct*. pp.2-9, The Catholic University of America, 1970.

2. Kuznetsov, V.K., Method of Virtual Sources in the Underwater-Acoustical Description of High-Frequency Sound Fields in a Wedge. *Soviet Physics Acoustics*, 18, No 2, pp223-228, OCT- DEC 1972.

3. Coppens, A.B., Sanders, J.V., Ioannou, I., and Kawamura, W., Programs for the Evaluation of the Acoustic Pressure Amplitude and Phase at the Bottom of a Wedge-Shaped Fluid Layer Overlying a Fast Fluid Half Space. Naval Postgraduate School Report 61-79-002, december 1978.

4. Jensen, F.B., and Kuperman, W.A., Sound Propagation in a Wedge- Shaped Ocean with a Penetrable Bottom. *Jour. Acoust. Soc. Am.*, 67(5), pp1566, May 1980.

5. Lee, D. and Botseas, G., IFD: AnImplicit Finite-Difference Computer Model for Soving the Parabolic Equation, *NUSC Techical Report 6659*, May 1982.

6. Jager, L.E., *A Computer Program for Solving the Parabolic Equation using an Implicit Finite-Difference Solution Method Incorporating Exact Interface Conditions*, Master's Thesis, Naval Postgraduate School, Monterey, California, September 1983.

7. Coppens, A.B., Humphries, M., and Sanders, J.V., Propagation of Sound Out of a Fluid Wedge into an Underlying Fluid Substrate of greater Sound Speed. *Jour. Acoust. Soc. Am.*, 76(5), pp1456-1465, November 1984.

8. Baek, C.K., *The Acoustic Pressure in a Wedge-Shaped Water Layer Overlying a Fast Fluid Bottom*. M.S.Thesis, Naval Postgraduate School, Monterey, California, March 1984.

9. Lesesne, P.K., *Development of Computer Program using the Method of Image to Predict the Sound Field in a Wedge Overlying a Fast Fluid and Comparison with Laboratory Experiments*. M.S.Thesis, Naval Postgraduate School, Monterey, California, December 1984.

10. Kinsler, Frey, Coppens and Sanders, *Fundamentals of Acoustics*. John Wiley & Sons, Third Edition, 1982.

11. Coppens, A.B., Note on Sound Field in a Wedge-Shaped Medium, (Informal).

12. Personal Communication With A.B. Coppens and J.V. Sanders. Naval Postgraduate School, Monterey, California 93940, March 1989.

13. Li Yu Ming, *Acoustic Pressure Distribution on the bottom of a Wedge-Shaped ocean*, M.S.Thesis, Naval Postgraduate School, Monterey, California, December 1987.

14. Demetrios Paliatsos, *Computer Studies of Sound Propagation in a Wedge-Shaped Ocean with Penetrable Bottom*, M.S.Thesis, Naval Postgraduate School, Monterey, California, March 1989.

15. Kim. Jong Rok, *Comparison of Sound Pressure in a Wedge-Shaped Ocean as Predicted by an Image Method and PE Model*, M.S.Thesis, Naval Postgraduate School, Monterey, California, December 1990.

INITIAL DISTRIBUTION LIST

1.	Defence Technical Information Center Cameron Station Alexandria, Virginia 22304-6145	2
2.	Library Code 52 Naval Postgraduate School Monterey, California 93943-5002	2
3.	Dr. K.E.Woehler, Code PH/Wh Chairman, Department of Physics Naval Postgraduate School Monterey, California 93943-5002	1
4.	Dr. A.B.Coppens, Code PH/Cz Department of Physics Naval Postgraduate School Monterey, California 93943-5002	2
5.	Dr. J.V.Sanders, Code PH/Sd Department of Physics Naval Postgraduate School Monterey, California 93943-5002	2
6.	Lee, Kyung Taek Kyung Sang Namdo Chinhae City DongSang-Dong 3 Dong APT 204 Ho Seoul, Korea	6